DNA condensation and packaging

October 13, 2009

Professor Wilma K. Olson

Viral DNA - chain molecules in confined spaces

Viruses come in all shapes and sizes

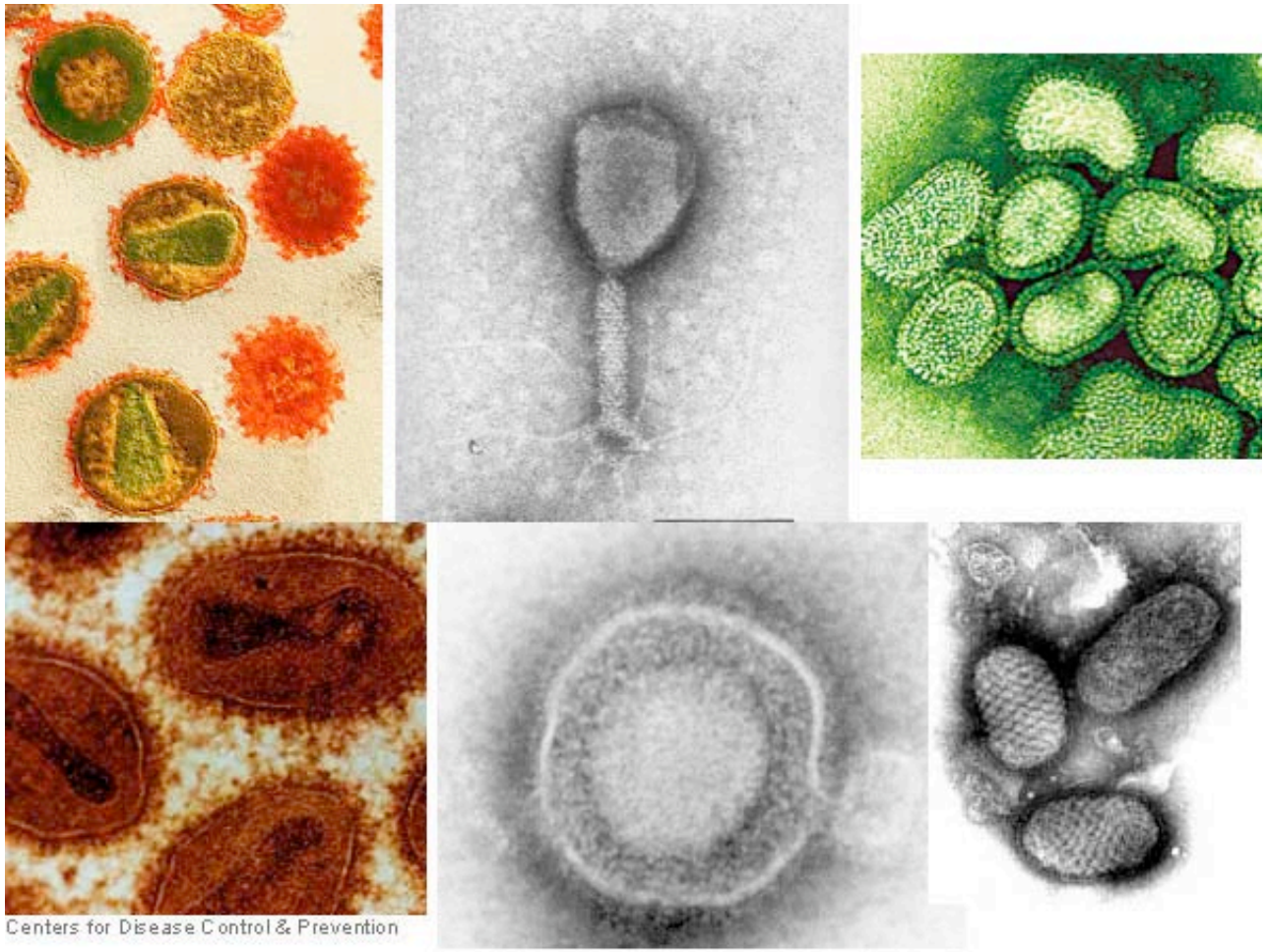

Clockwise: Human immuno deficiency virus (HIV); Aeromonas virus 31, Influenza virus, Orf virus, Herpes simplex virus (HSV), Small pox virus

Image from U Wisconsin Microbial World website: http://bioinfo.bact.wisc.edu

DNA packaging pathway of T3 and T7 bacteriophages

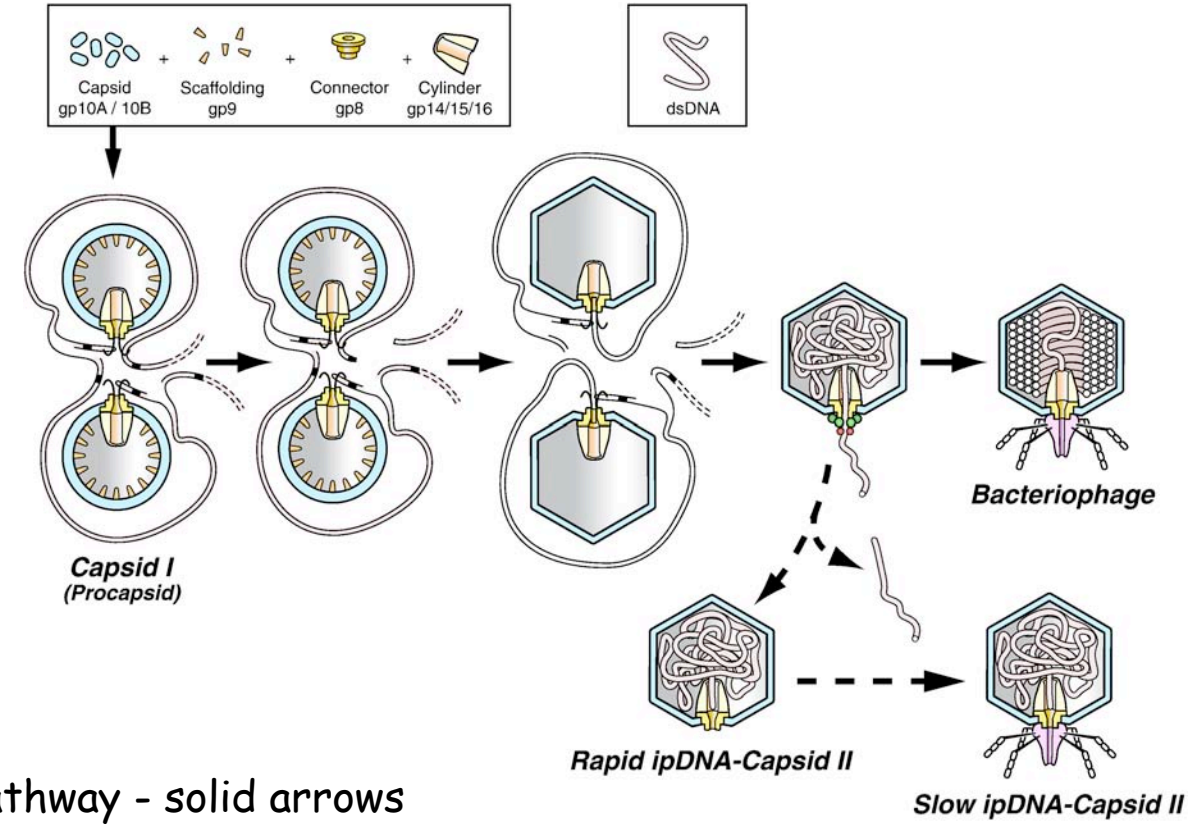

- *In vivo* pathway - solid arrows

Fang *et al.* (2008) "Visualization of bacteriophage T3 capsids with DNA incompletely packaged *in vivo.*" *J. Mol. Biol.* 384, 1384-1399

Cryo EM images of T3 capsids with 10.6 kbp packaged DNA

- Labels mark particles representative of different types of capsids
- Arrows point to tails on capsids

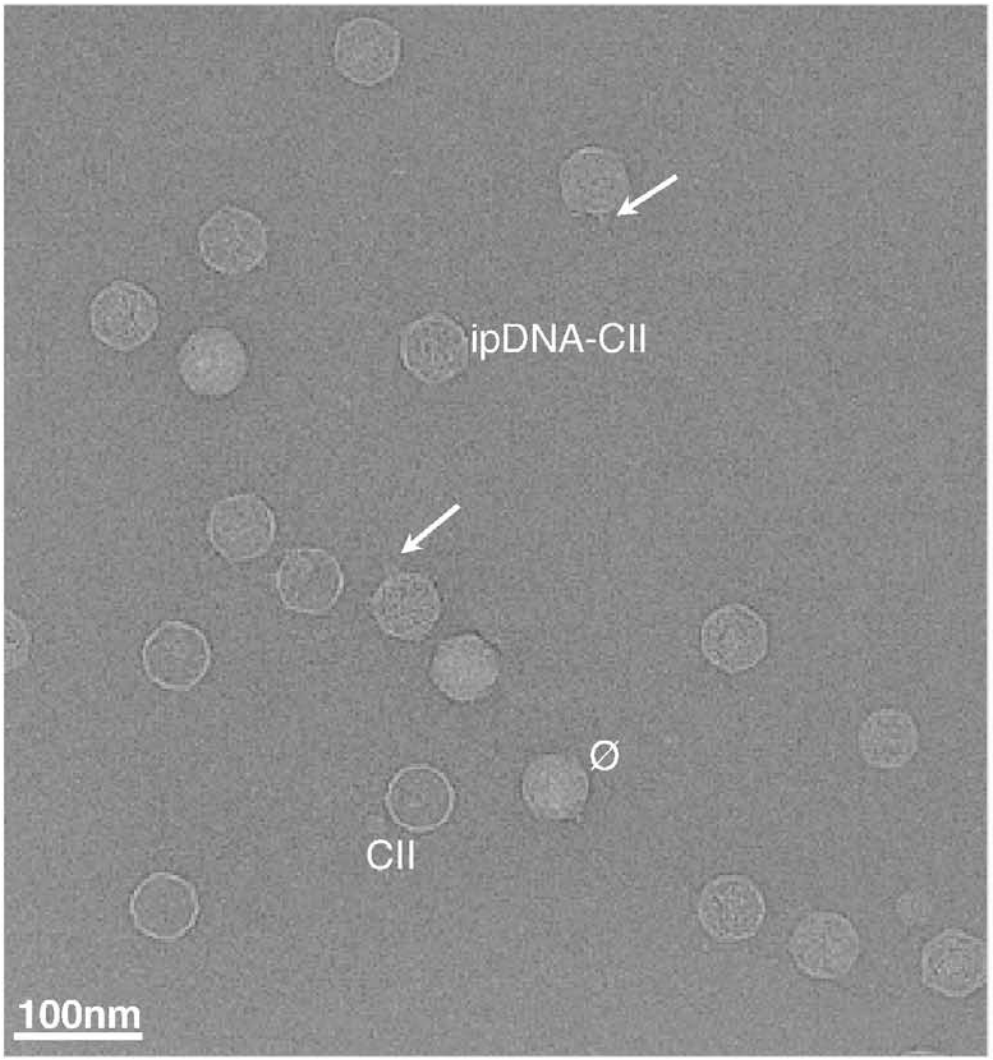

Fang *et al.* (2008) "Visualization of bacteriophage T3 capsids with DNA incompletely packaged *in vivo*."" *J. Mol. Biol.* 384, 1384-1399

Cryo EM images of representative particles

- (b) 10.6 kbp DNA
- (c) 22 kbp DNA
- (d) bacteriophage T3

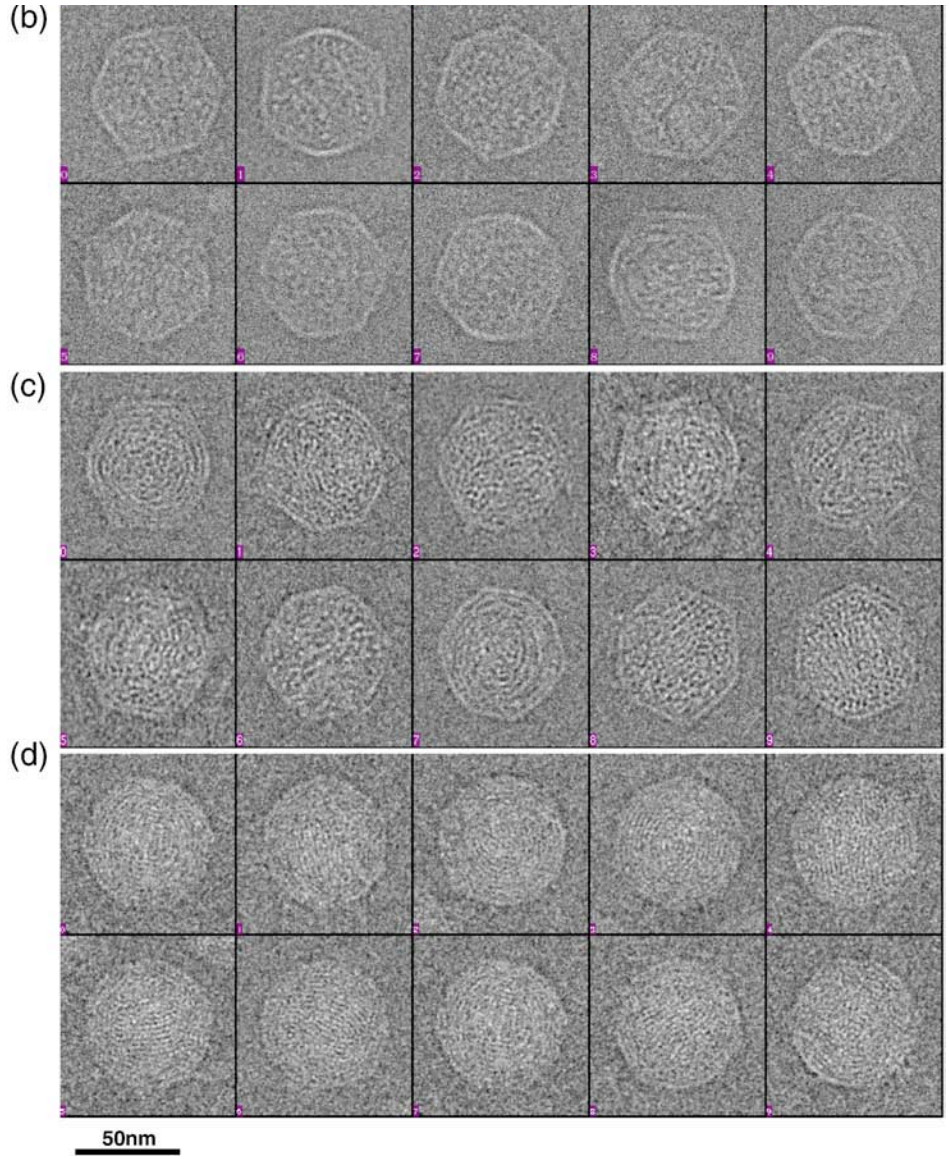

Fang *et al.* (2008) "Visualization of bacteriophage T3 capsids with DNA incompletely packaged *in vivo*." *J. Mol. Biol.* 384, 1384-1399

3D icosohedral reconstructions of cryo-EM-imaged particles

Threefold surface views and central cross sections

- (b) 10.6 kbp DNA
- (c) 22 kbp DNA
- (d) bacteriophage T3

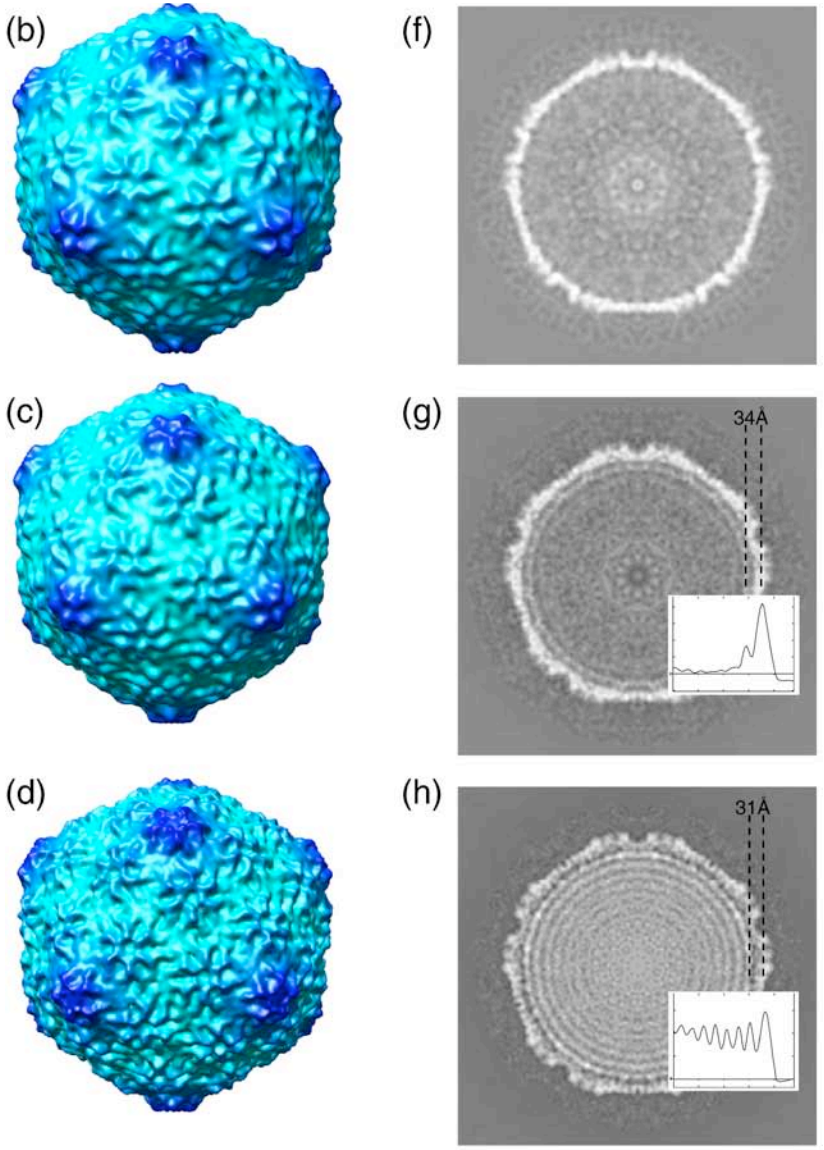

Fang *et al.* (2008) "Visualization of bacteriophage T3 capsids with DNA incompletely packaged *in vivo*." *J. Mol. Biol.* 384, 1384-1399

Top-down views of λ phage DNA toroids captured in cryo-EM micrographs

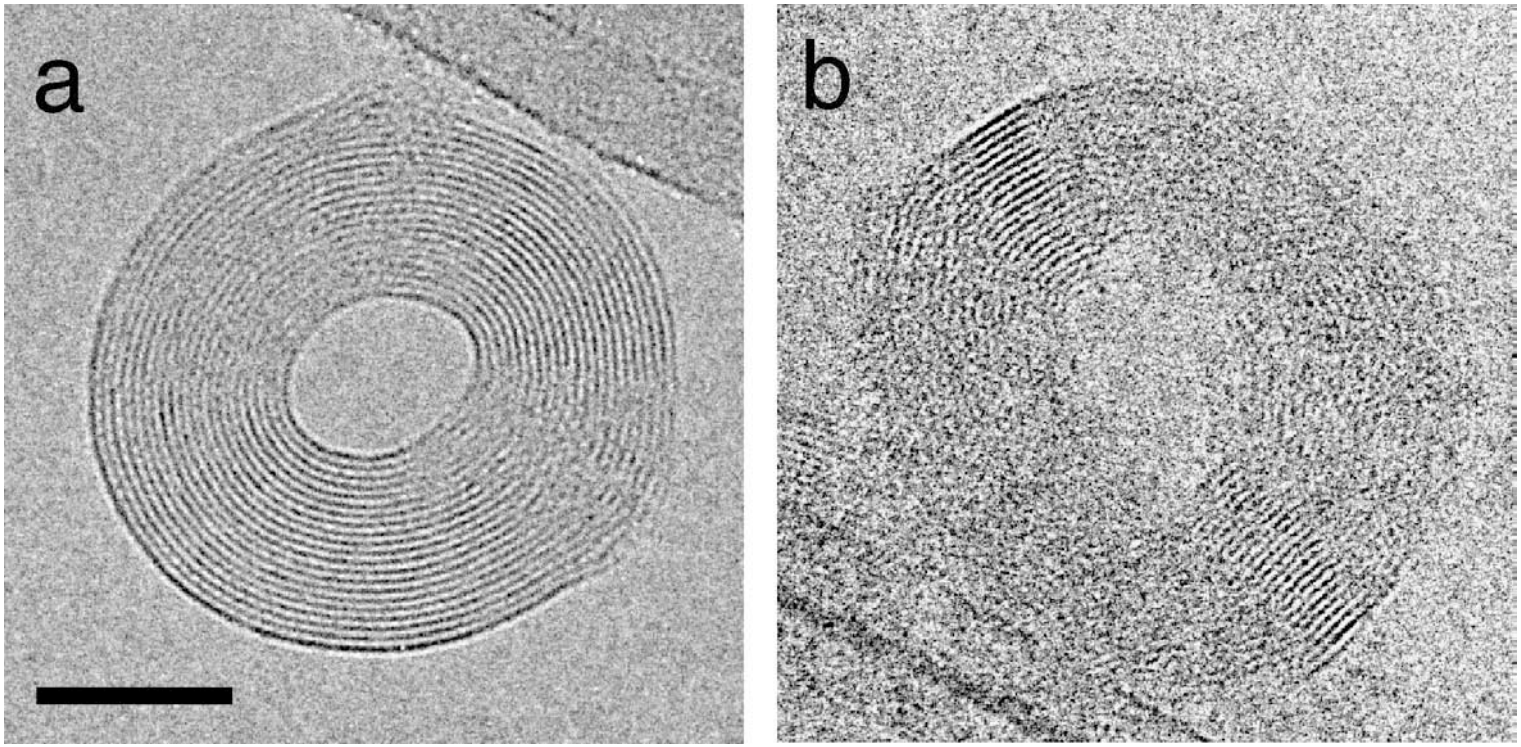

Note the circumferential winding of DNA found in collapsed toroidal particles produced in the presence of multi-valent cations.

Hud & Vilfan (2005) "Toroidal DNA condensates: unraveling the fine structure and the role of nucleation in determining size." *Ann. Rev. Biophys. Biomol. Struct.* 34, 295-318

Images of DNA toroids produced in the presence of hexammine cobalt chloride

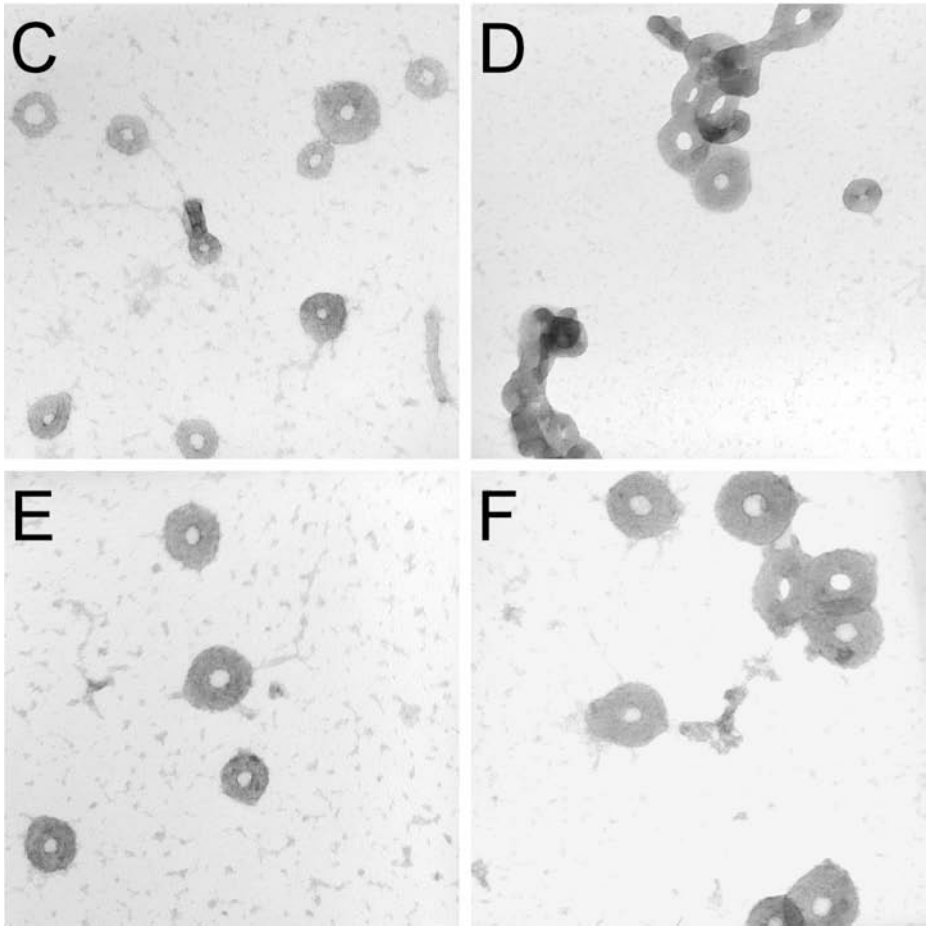

3 kbp DNA condensed from (C) 2.5 mM NaCl ; (D) 1.75 mM $MgCl_2$; (E) 3.75 mM NaCl; (F) 2.5 mM $MgCl_2$

Hud & Vilfan (2005) "Toroidal DNA condensates: unraveling the fine structure and the role of nucleation in determining size." *Ann. Rev. Biophys. Biomol. Struct.* 34, 295-318

Images of T4 DNA toroids produced in the presence of spermidine in high salt

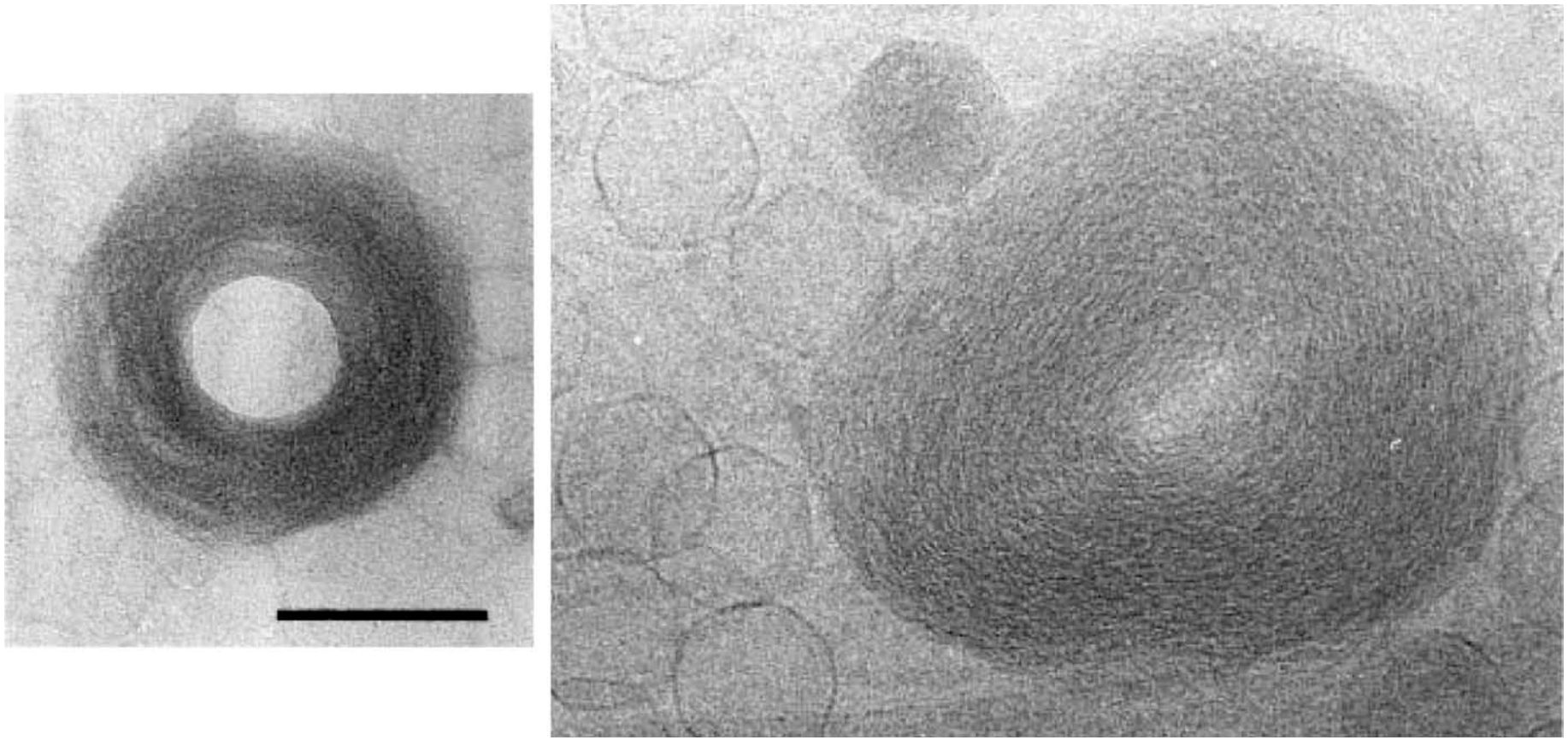

Note size of free toroids, formed by release of DNA from bacteriophages in solution of spermidine and high salt, compared to empty and DNA-filled bacteriophages.

Hud & Vilfan (2005) "Toroidal DNA condensates: unraveling the fine structure and the role of nucleation in determining size." *Ann. Rev. Biophys. Biomol. Struct.* 34, 295-318

Toroid size depends on DNA sequence.

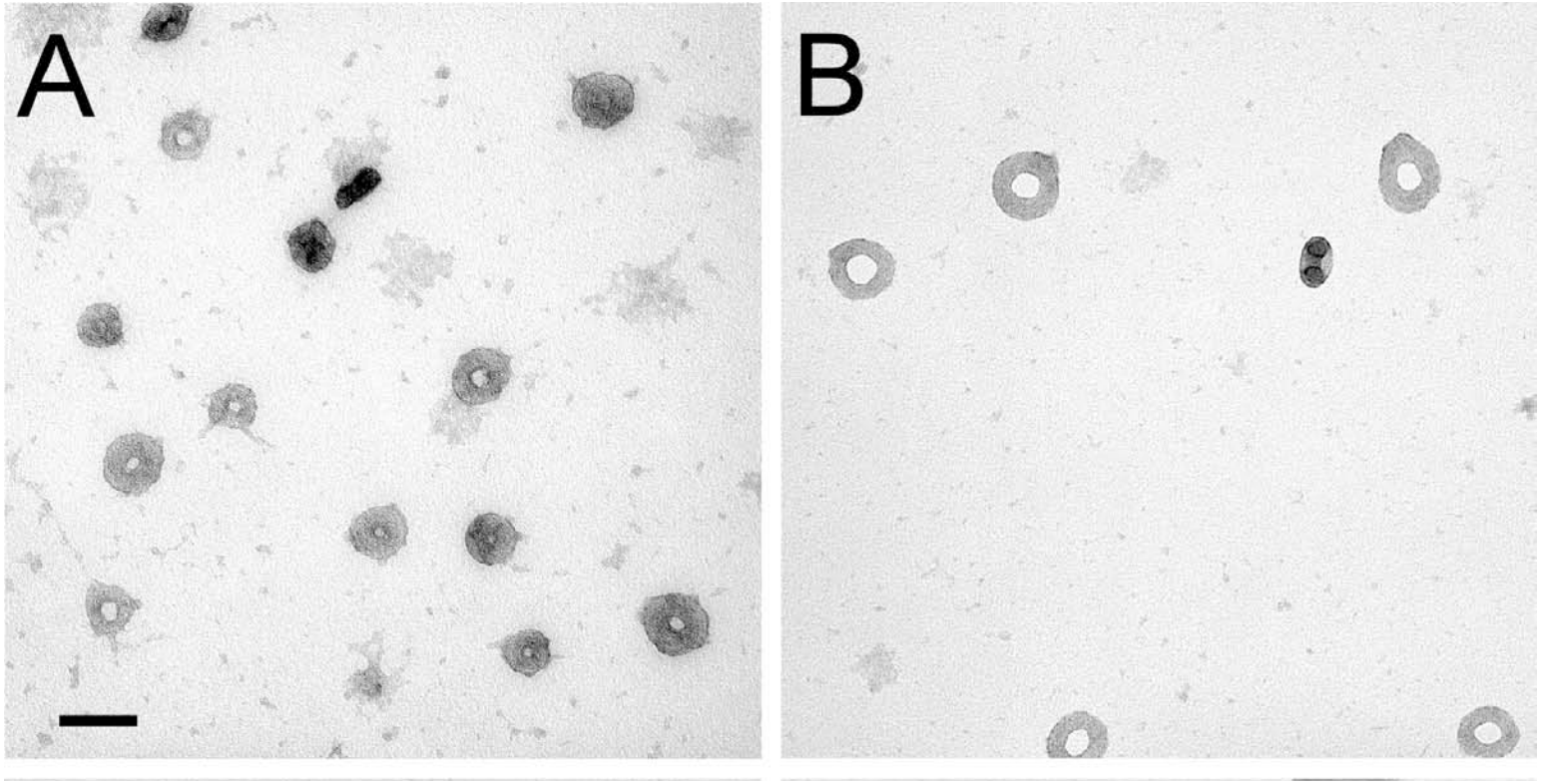

Note smaller size of toroids (A) produced by 3 kbp DNA with extensive sequence directed curvature vs.. (B) control 3 kbp sequences without such curvature.

Hud & Vilfan (2005) "Toroidal DNA condensates: unraveling the fine structure and the role of nucleation in determining size." *Ann. Rev. Biophys. Biomol. Struct.* 34, 295-318

The packing of helices in high-resolution structures hints of how DNA might pack inside a viral capsid.

B-DNA packing motifs

- G in minor groove of one helix H bonds with G in the minor groove of another, as in the Dickerson-Drew dodecamer.
- Helices stack on top of one another with the phosphates forming lateral interactions.
- Bases in the major groove of one helix interact with the phosphate backbone of another

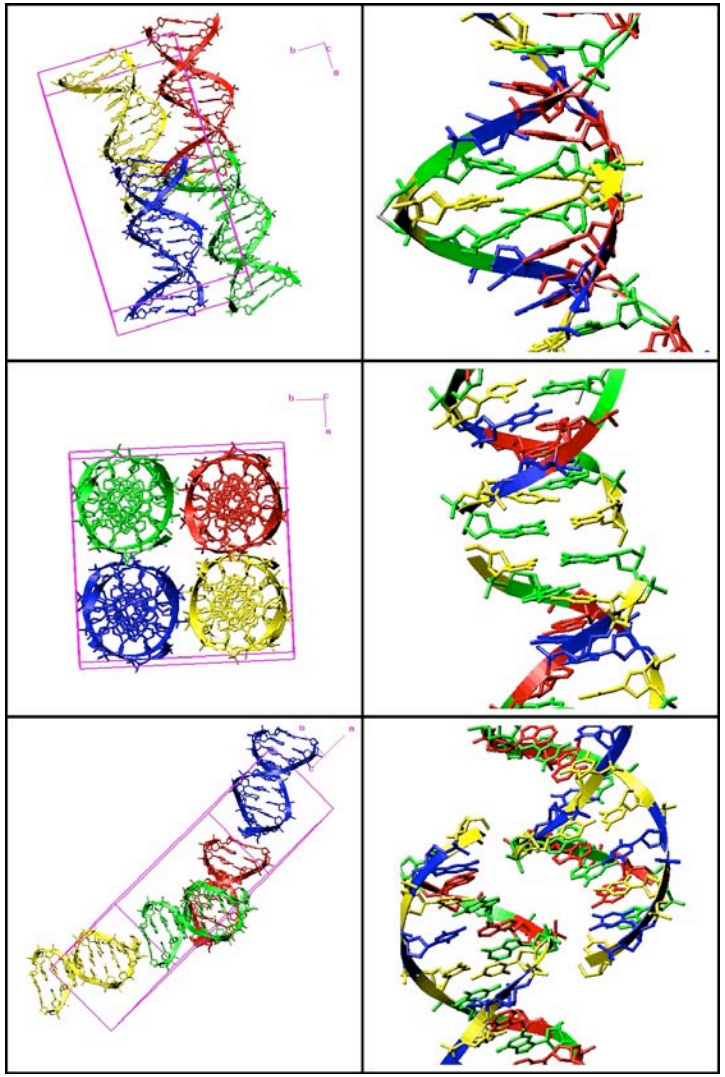

Berman & Olson (2003) "The many twist of DNA." in *DNA50: The Secret of Life*, Faircount LLC, London, pp. 104-124

Adjacent gyres of DNA wrapped on the nucleosome core particle form a 'supergroove' that accommodates the binding of a long polyamide 'clamp'.

(a)

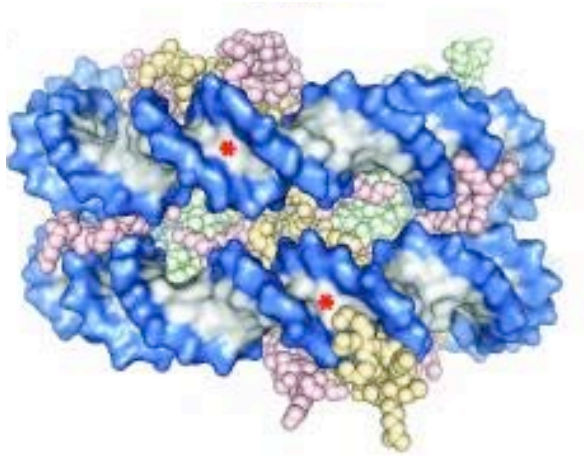

Side view of the nucleosome core particle highlighting the DNA 'super' major and minor (*) grooves formed by nucleotides separated by a complete superhelical turn.

DNA: sugar-phosphate backbone (blue), bases (white). Histone proteins: H2A (yellow), H2B(pink); H3 (blue); H4(green)

(b)

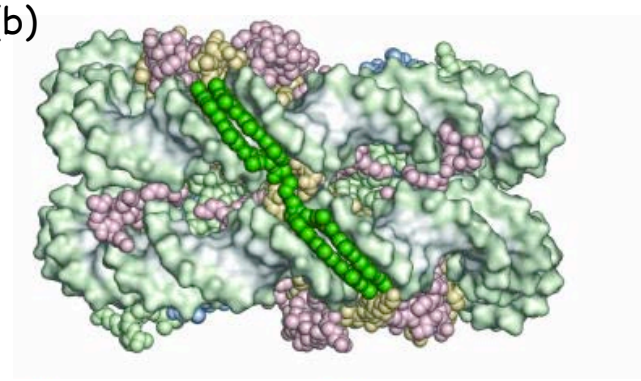

Clamp binding in the nucleosomal-polyamide crystal complex (PDB ID 1s32). Orientation and color coding of histone proteins as in (a). DNA: sugar-phosphate backbone (green), bases (white).

Polyamide atoms: dark green.

Edayathumangalam *et al.* (2004) "Molecular recognition of the nucleosomal "supergroove"." *Proc. Natl Acad. Sci., USA* 101, 6864–6869.

Homologous DNA sequences appear to recognize on another in liquid-crystal aggregates.

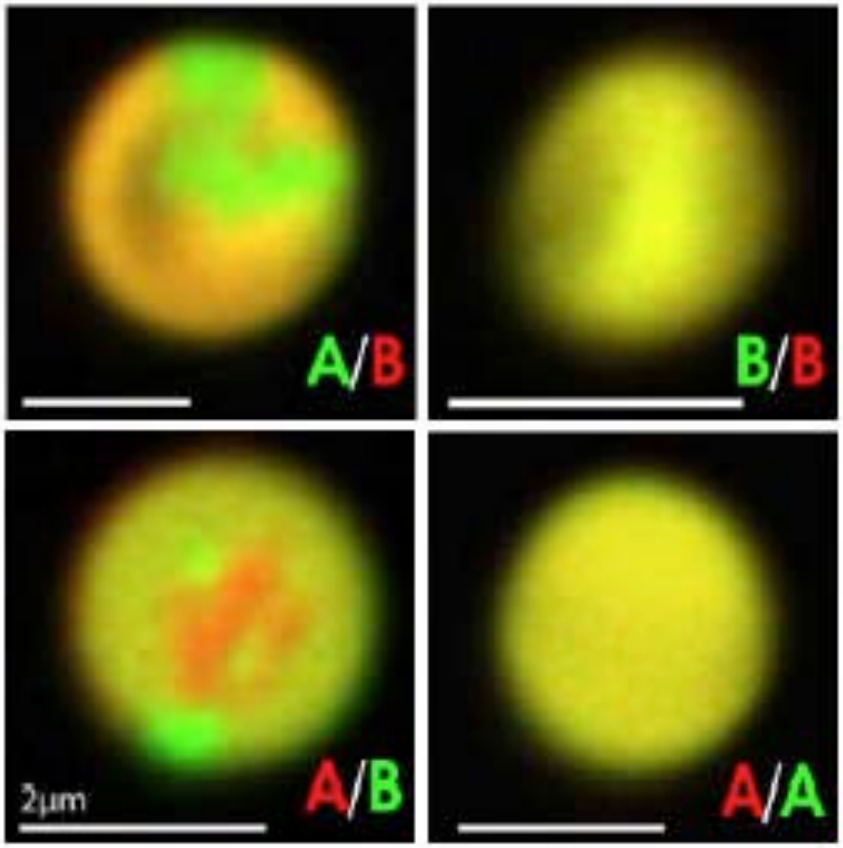

Two 294-bp DNA molecules of comparable nucleotide composition spontaneously segregate in liquid-crystalline aggregates. Fragments A and B labeled with different dyes (1 dye per 25 DNA).

Baldwin *et al.* (2008) "DNA double helices recognize mutual sequence homology in a protein free environment" *J. Phys. Chem. B* 112, 1060-1064.

Kornyshev-Leikin theory of interaction between helical molecules is potentially applicable to problems of DNA compaction.

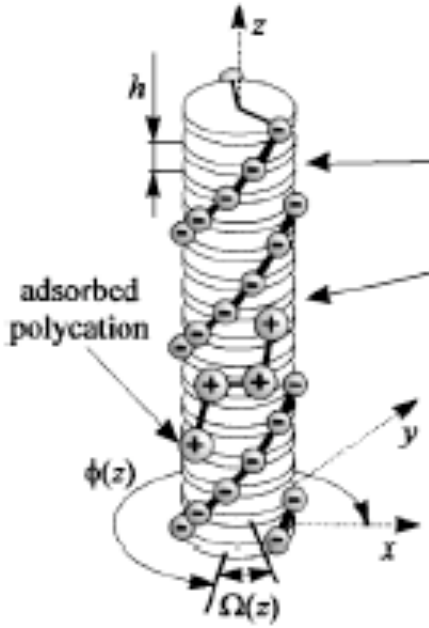

a

B DNA represented as a stack of bps with two negatively charged phosphate groups and adsorbed major-groove-bound polycations

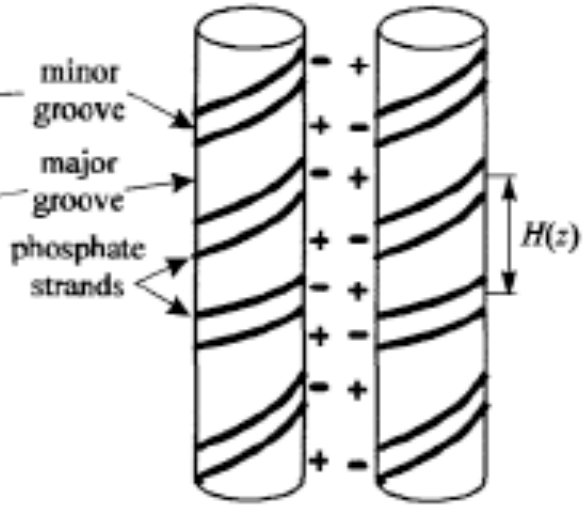

b

Sequence-dependent twist modulations lead to variation in helical pitch $H(z)$. So that only homologous sequences can have negatively charged strands facing positively charged grooves of another DNA.

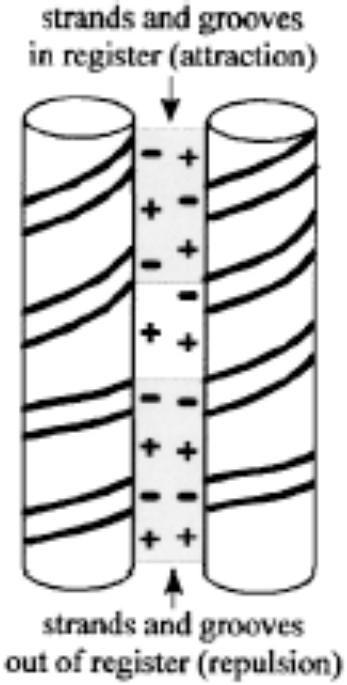

c

Molecules with unrelated sequences result in the loss of register between the strands and grooves in opposing molecules.

Kornyshev & Leikin (2001) "Sequence recognition in the pairing of DNA duplexes" *Phys. Rev. Lett.* 86, 3666-3669.

Bacterial DNA - chain molecules anchored and decorated by proteins

Many protein assemblies bind sequentially distant sites on bacterial genomes, forcing the intervening DNA into a protein-mediated loop.

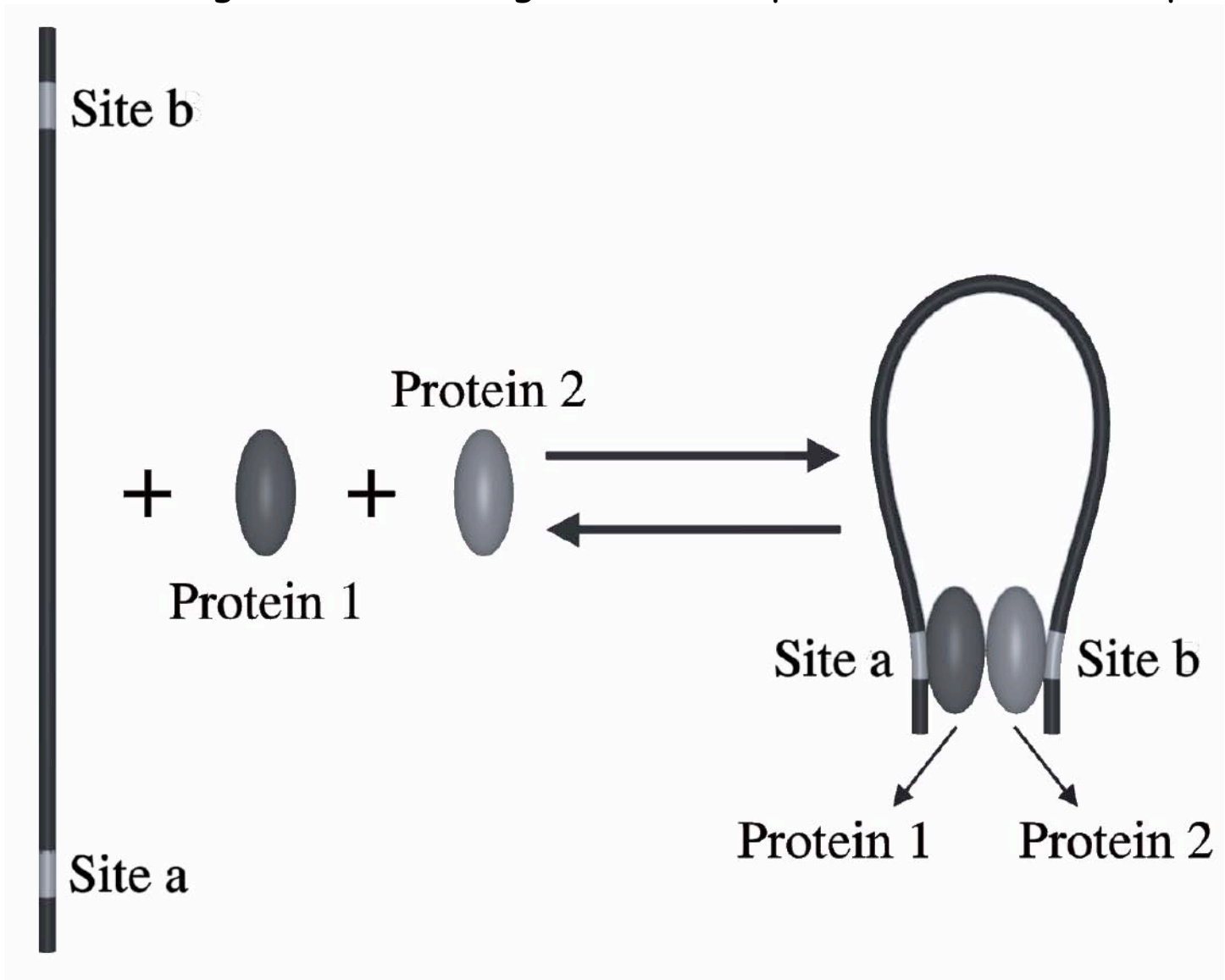

The tetrameric Lac repressor protein assembly represses the expression of the *lac* operon by simultaneously binding to two DNA sites in the vicinity of the nucleotides at which transcription starts.

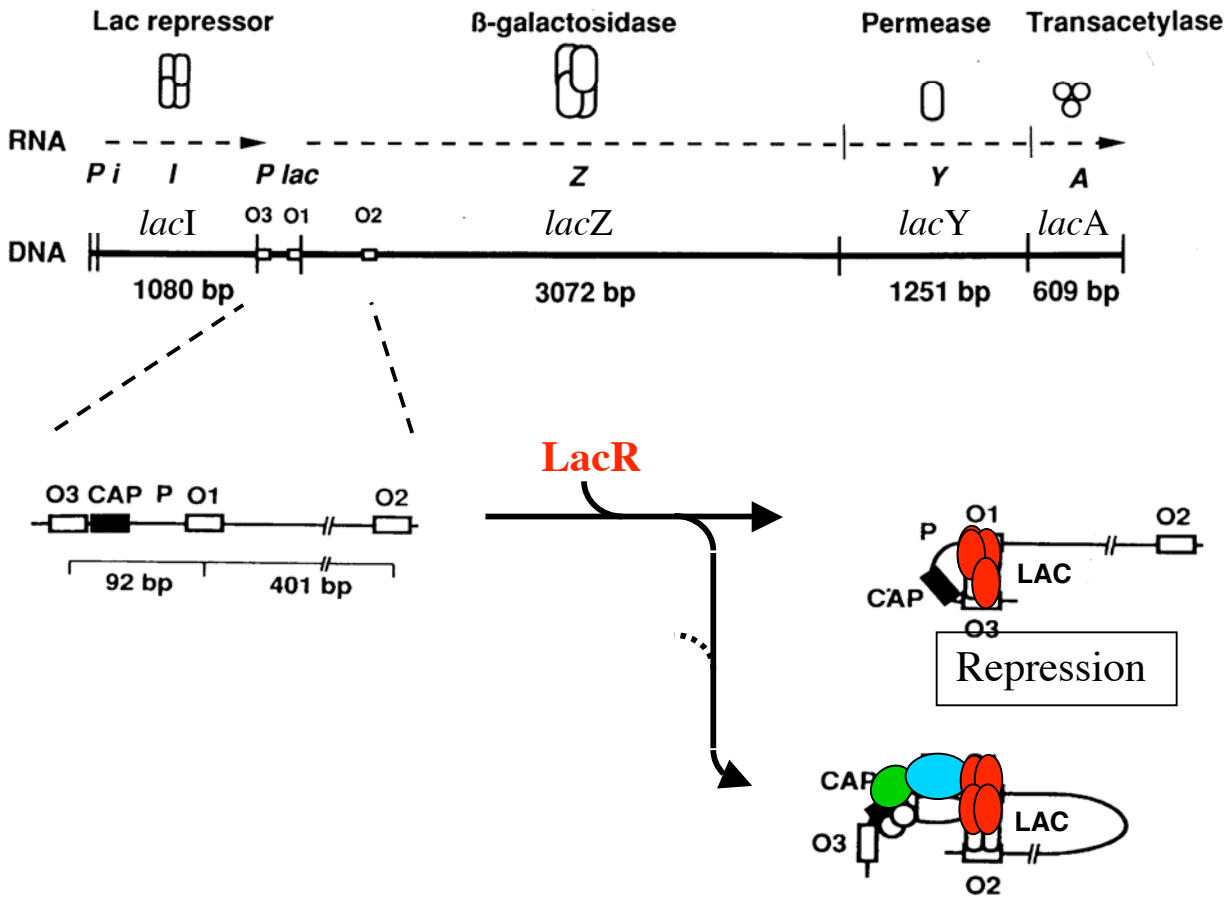

The binding of the Lac repressor protein to the *lac* operotor is thought either to inhibit the binding of RNA polymerase at the promoter site or to block the movement of RNA polymerase along DNA.

The non-specificity the HU protein seemingly affects the looping of DNA

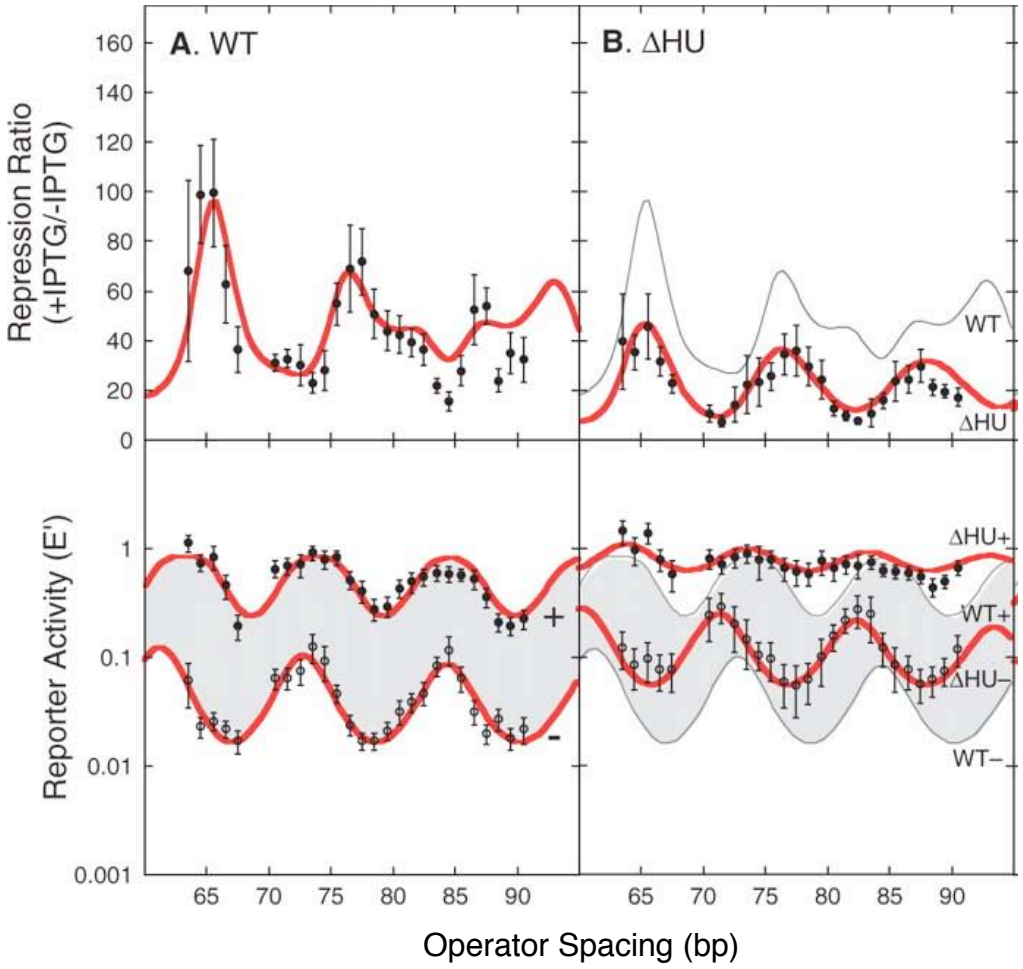

DNA looping properties in *E. coli*, measured by the expression levels of a *lacZ* reporter gene.
Loss of HU disables looping (repression ratios lower than in wild-type cells)

Becker *et al.* (2007) "Effects of nucleoid proteins on DNA repression loop formation in *Escherichia coli*," *Nucleic Acids Res.* **35**, 3988-4000.

High-resolution structures provide insight into the fluctuations and specificity of the complex of DNA with the binding headpiece and the relative position of DNA with respect to the dimeric protein assembly.

PDB_ID 2bjc

Salinas *et al.* (2005)
"NMR structure of a protein-DNA complex of an altered specificity mutant of the Lac repressor that mimics the Gal repressor."
Chembiochem. 6, 1628-1637.

PDB_ID 1osl

Kalodimos *et al.* (2004)
"Solution structure of a dimeric lactose DNA-binding domain complexed to a nonspecific DNA sequence ."
Science 305, 386-389.

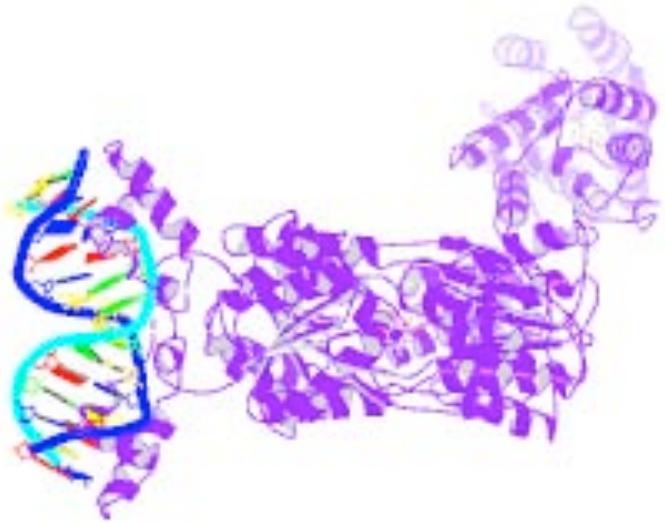

PDB_ID 1jwl

Bell & Lewis (2001)
"Crystallographic analysis of Lac repressor bound to natural operator O1."
J. Mol. Biol. 312, 921-926.

The 4.8-Å structure of the DNA-tetramer complex provides insight into the relative spatial positions of distant binding sites.

(PDB_ID 1lbg; Lewis *et al. Science* 271, 1247-1254, 1996)

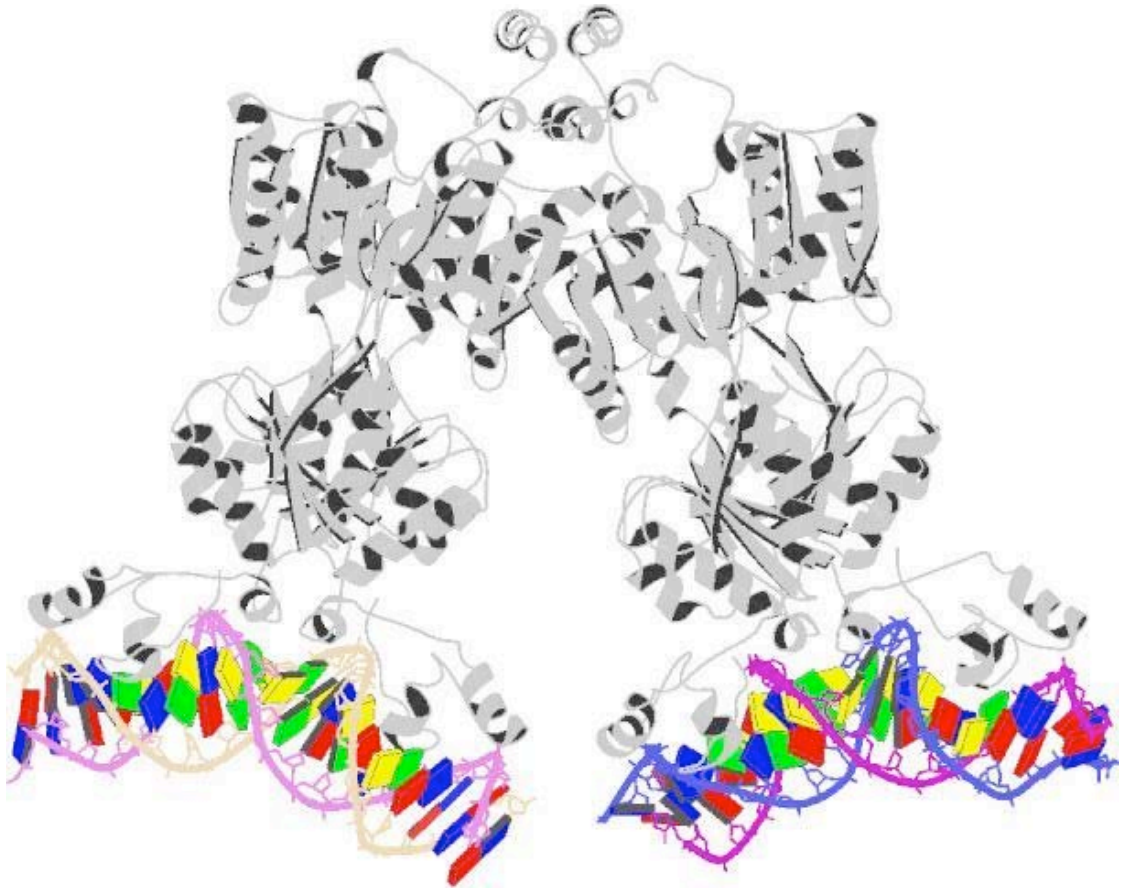

5´-AATTGTGAGCGCTCACAATT->3´ … 79 bp … **5´-AATTGTGAGCGCTCACAATT->3´**
3´<-TTAACACTCGCGAGTGTTAA-5´ **3´<-TTAACACTCGCGAGTGTTAA-5´**

Palindromic recognition sequence

The O1 and O3 operators can be oriented in two ways on LacR, with the coding strand pointed toward the interior or the exterior of the assembly.

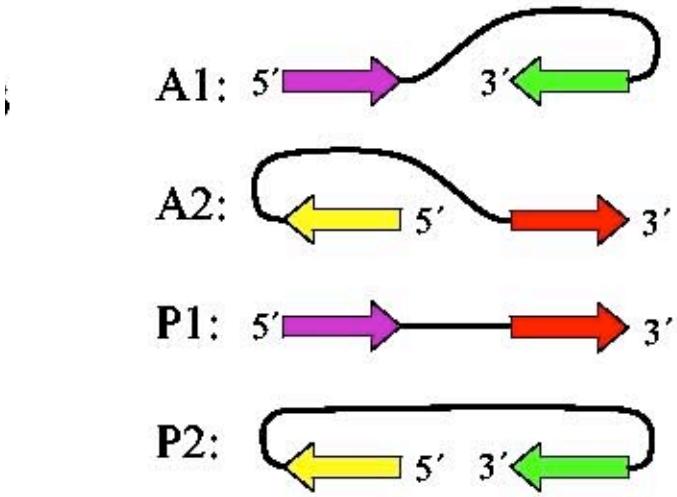

The combination of orientations gives rise to four possible loop types: two antiparallel (A1, A2) and two parallel (P1, P2) (Geanacopoulos *et al.*, 2001)

Antiparallel configurations of the wild-type loop are favored over parallel forms.

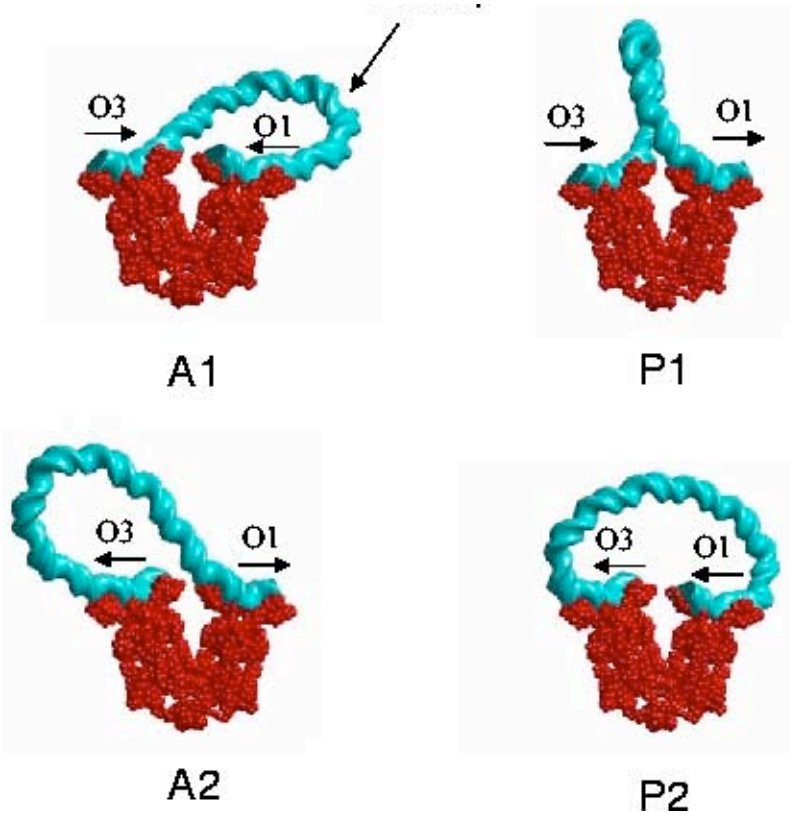

Loop	G_{DNA}	G_{DNA}
	100 mM	10 mM
A1	55.3	90.5
A2	55.8	90.9
P1	60.0	96.6
P2	69.1	104.1

Swigon *et al.* (2005) "Modeling the Lac repressor-operator assembly: the influence of DNA looping on Lac repressor conformation." *Proc. Natl. Acad. Sci., USA* 103, 9879-9884.

The simulated likelihood of loop formation in the presence of HU mimics the complex, chain-length dependent expression of genes controlled by LacR.

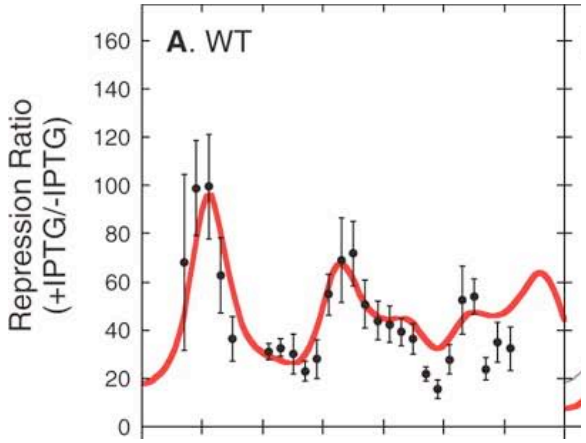

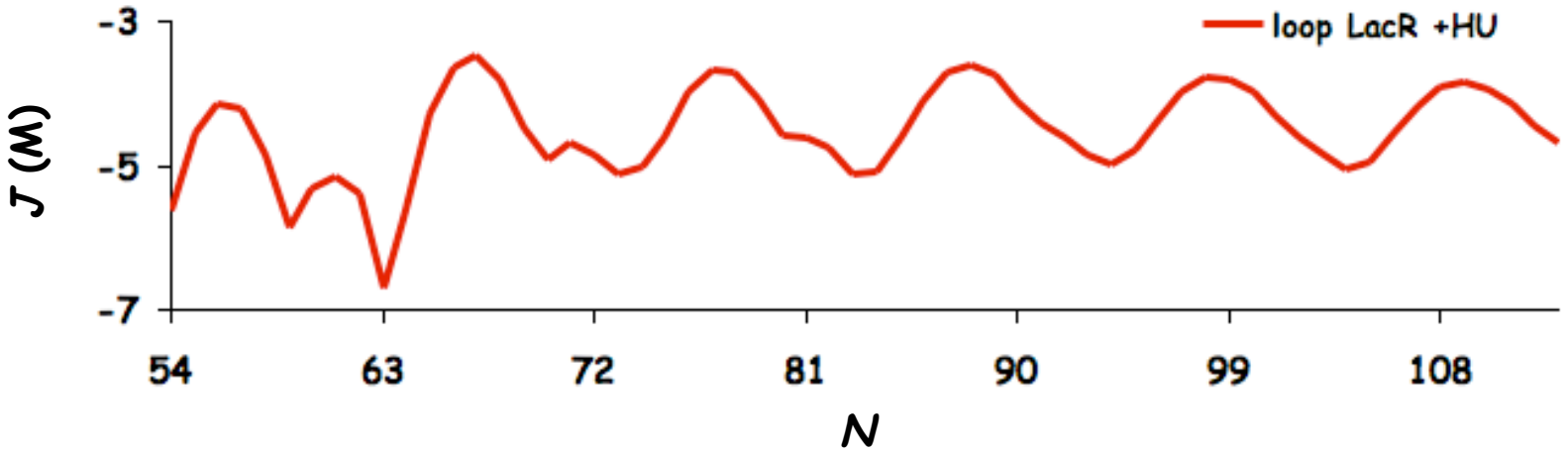

The simulated bimodal pattern of looping mediated by LacR and HU reflects the propensity of DNA to adopt different types of loops at different chain lengths.

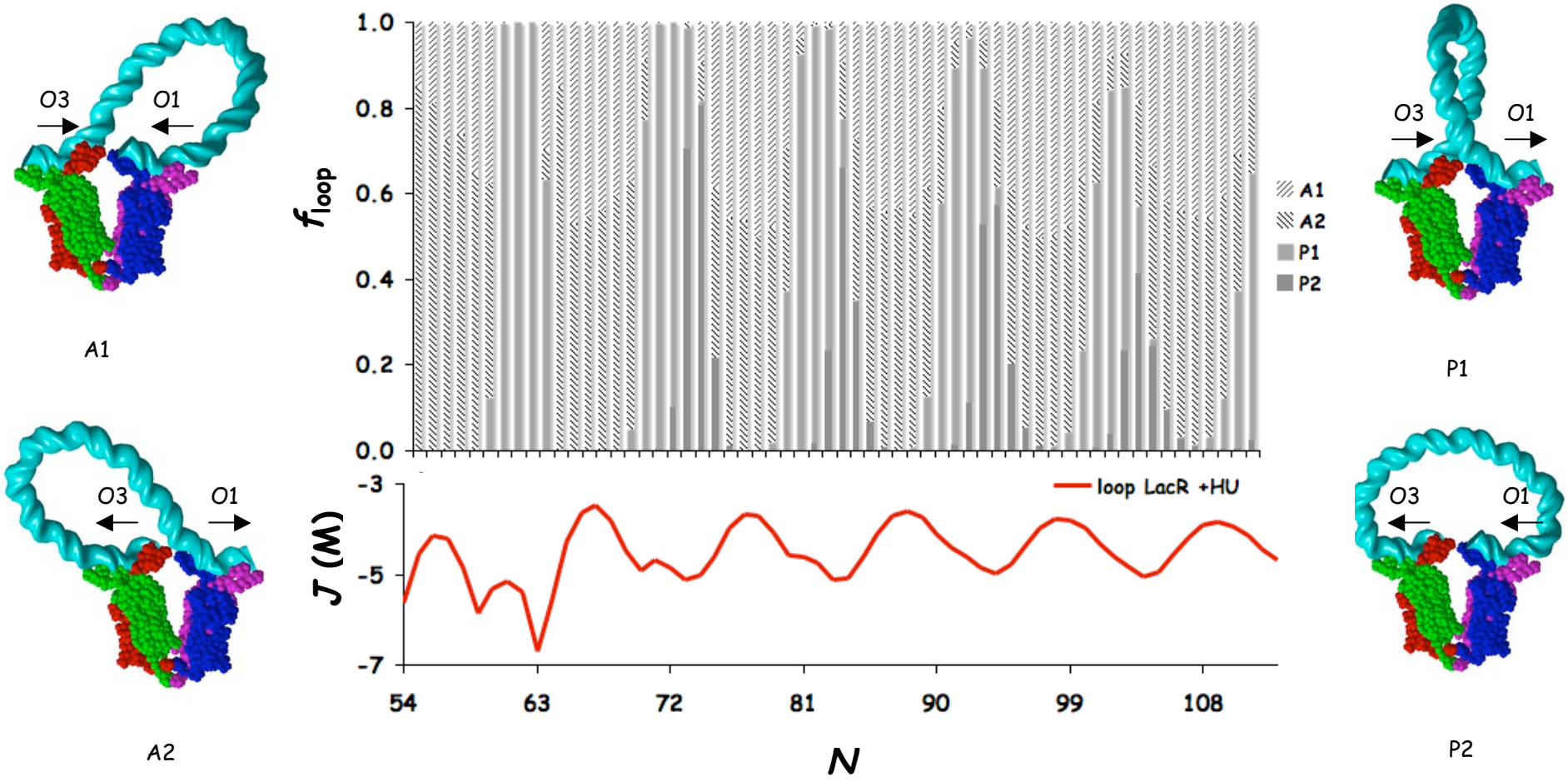

Minimum-energy configurations of DNA fragments complexed with the crystalline V-shaped LacR tetramer assembly (Swigon *et al.*, 2006)

The histone-like heat-unstable HU protein bends DNA by ~140°.

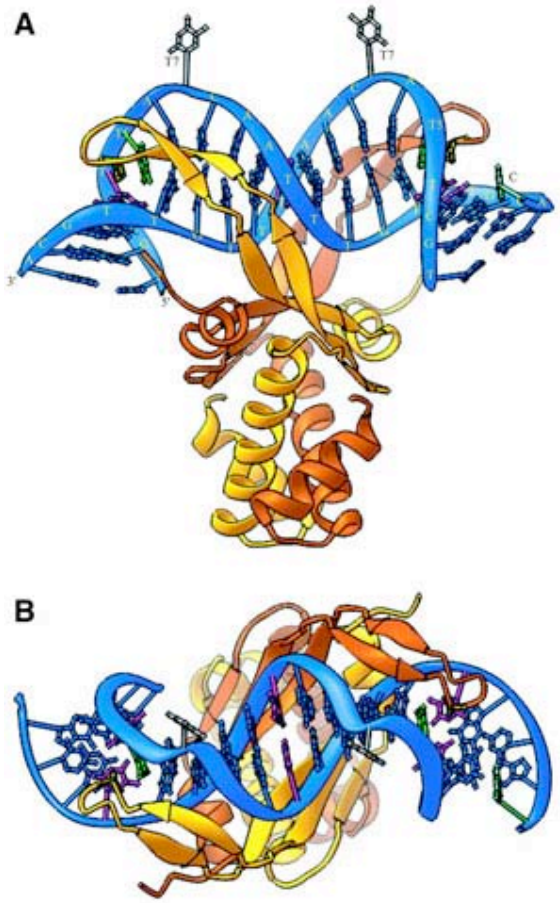

Color-coded representations of the HU homodimeric protein from the cyanobacterium *Anabaena* PCC7120 bound to DNA: NDB_IDs: pd0426, pd0430, pd0431.

Swinger *et al* (2003)"Flexible DNA bending in HU-DNA cocrystal structures," *EMBO. J.* **22**, 3749-3760

HU builds up at apical sites on LacR-mediated DNA loops.

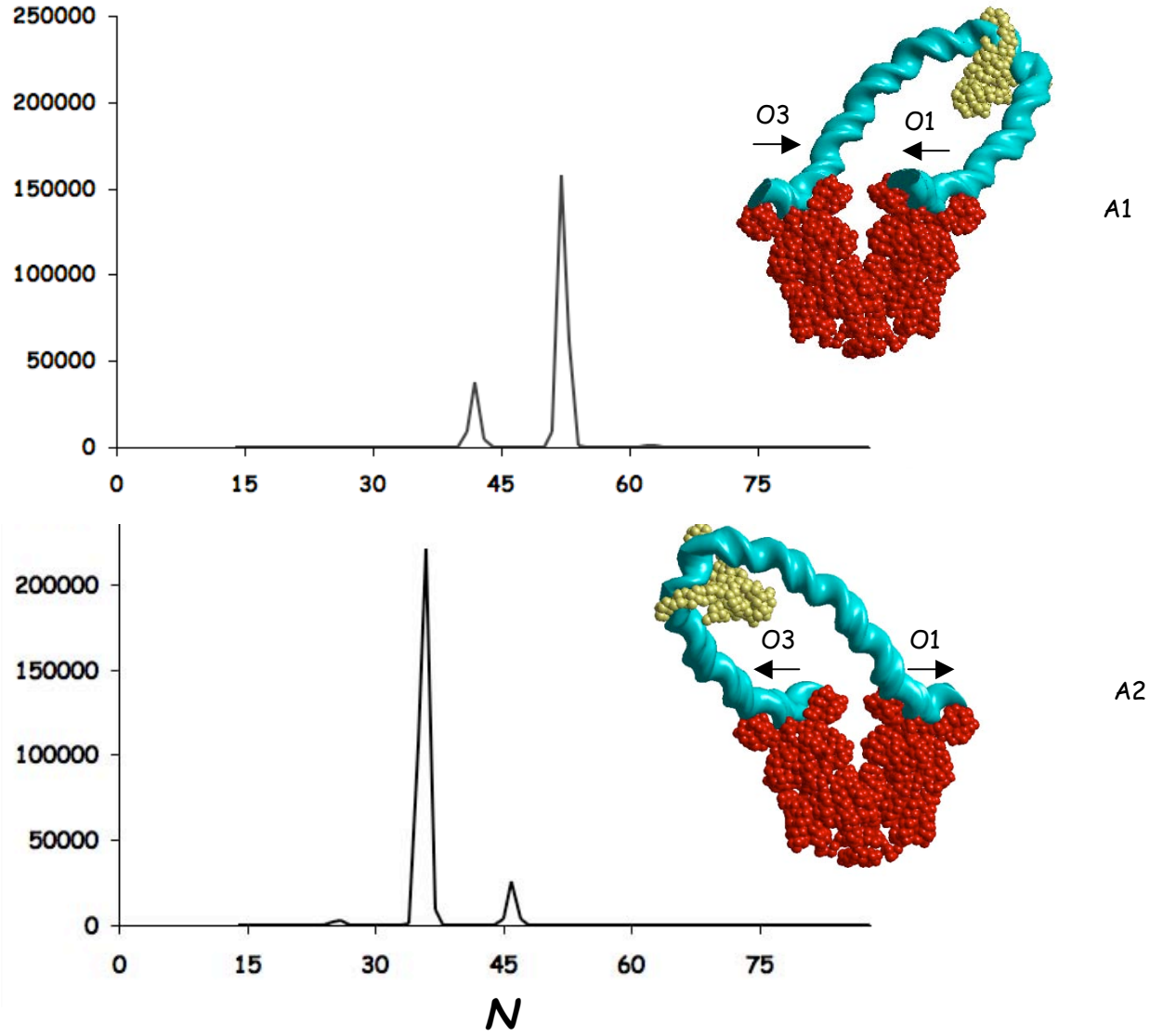

A1 and A2 loops (88 bp) bind 1 HU at their apexes, respectively 60% and 40% along the chain contour.

Eukaryote DNA - chain molecules wrapped around histone octamers

The nucleosome core particle is one of the most striking examples of protein-induced DNA deformation.

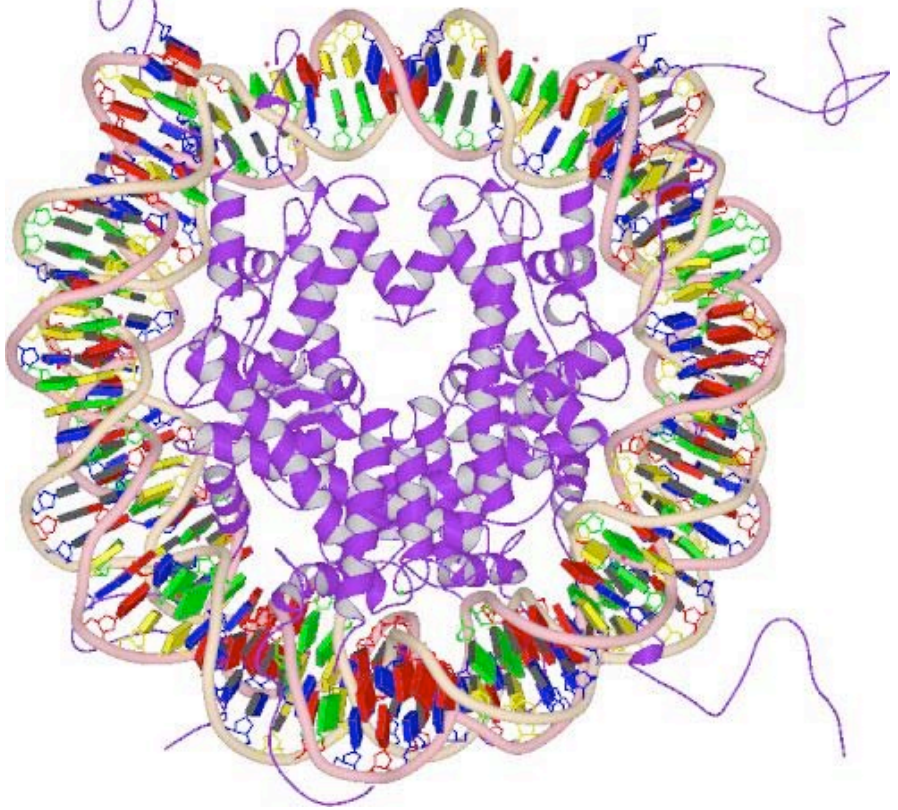

Simplified, color-coded representation of a 147 base-pair DNA wrapped ~1.6 turns around a (violet) core of eight proteins in the nucleosome core particle, the fundamental DNA packaging unit in eukaryotes: PDB_ID: 1kx5 (Davey *et al.*, 2002)

DNA wraps around an assembly of eight proteins, two of each of four histones.

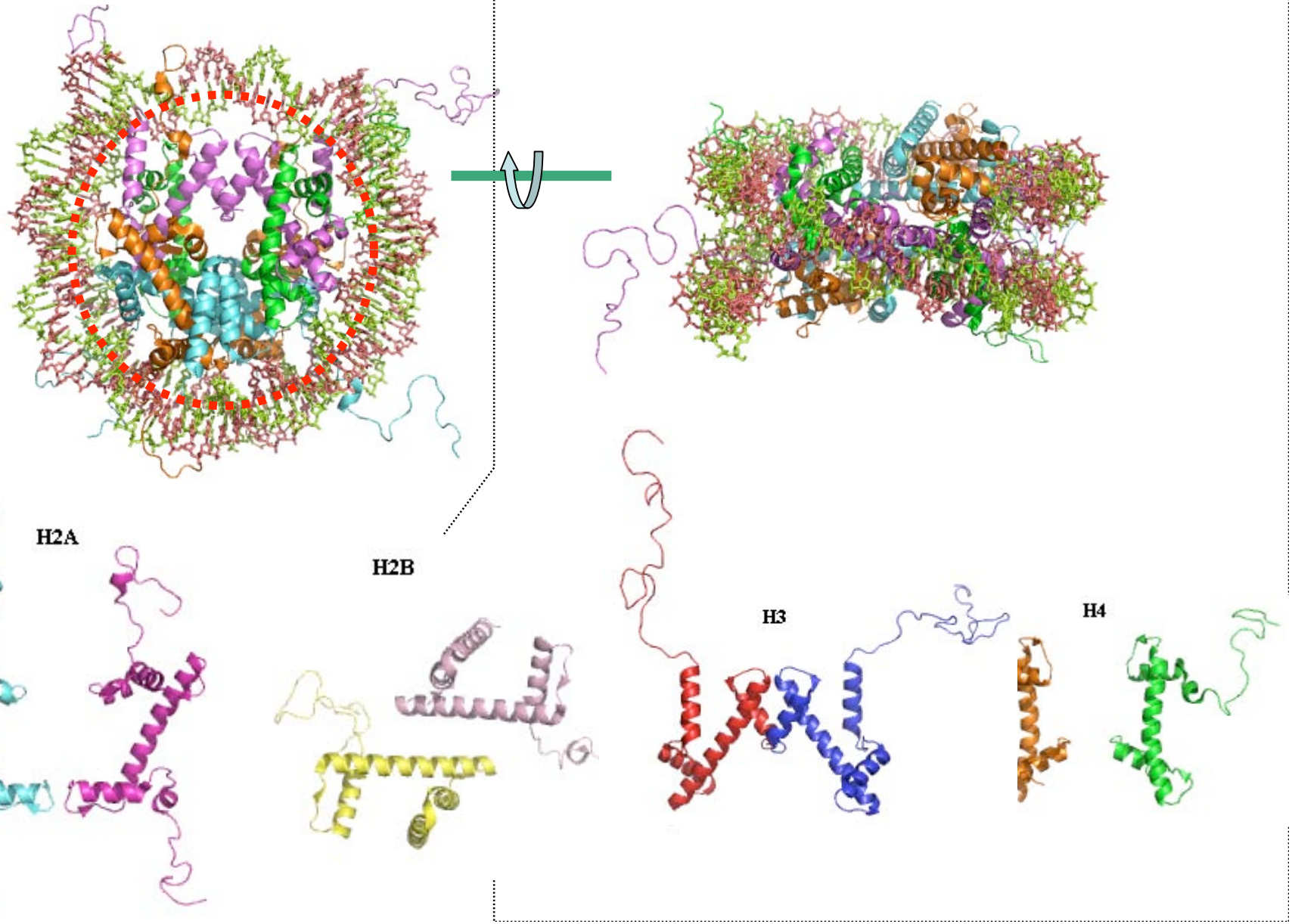

The histones adopt a common folding motif - the 'histone fold'

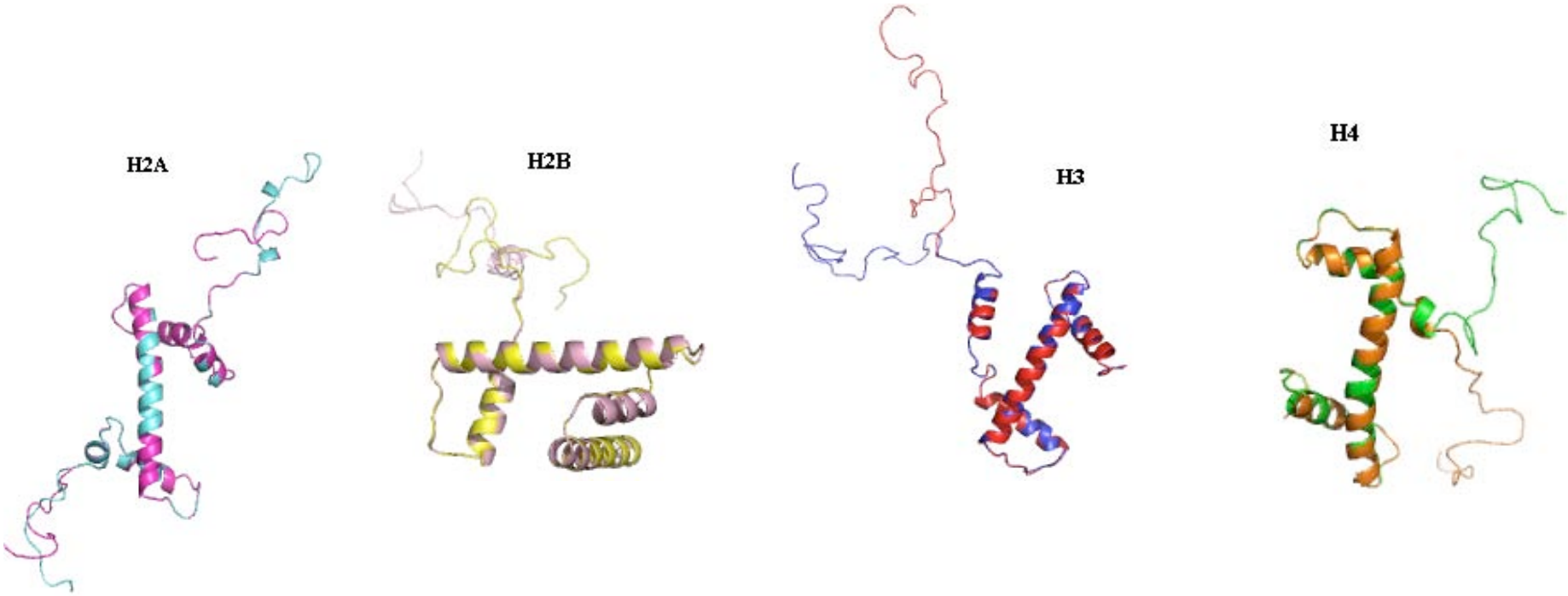

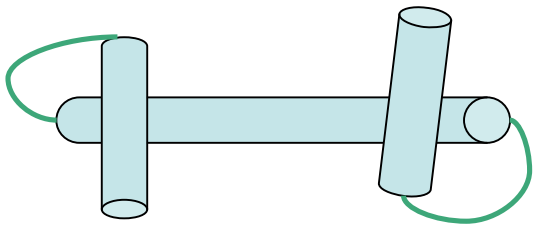

Histone pairs (H3/H4 and H2A/H2B) dimerize via a head-tail 'handshake' motif.

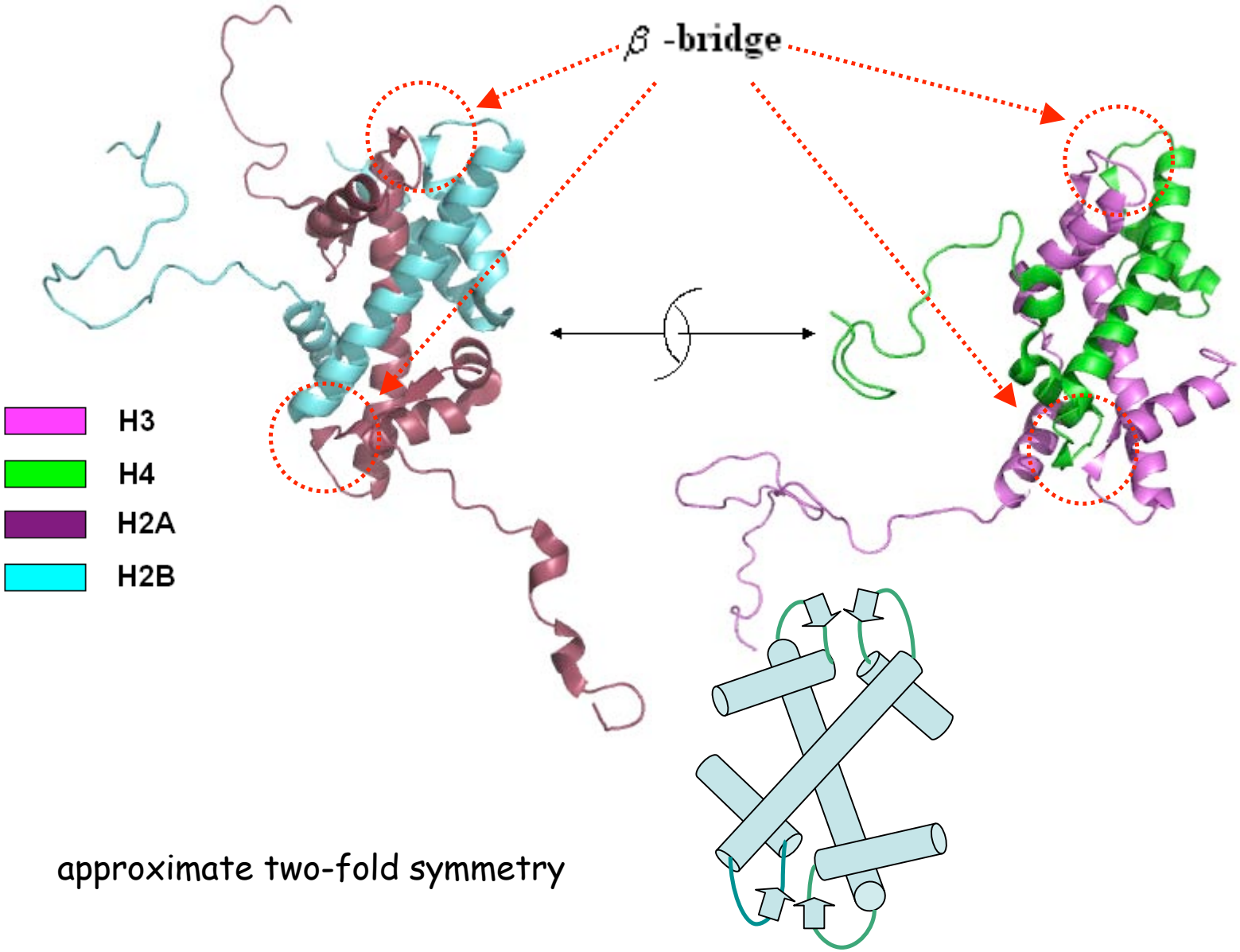

approximate two-fold symmetry

Histones H3 and H4 assemble as a tetramer.

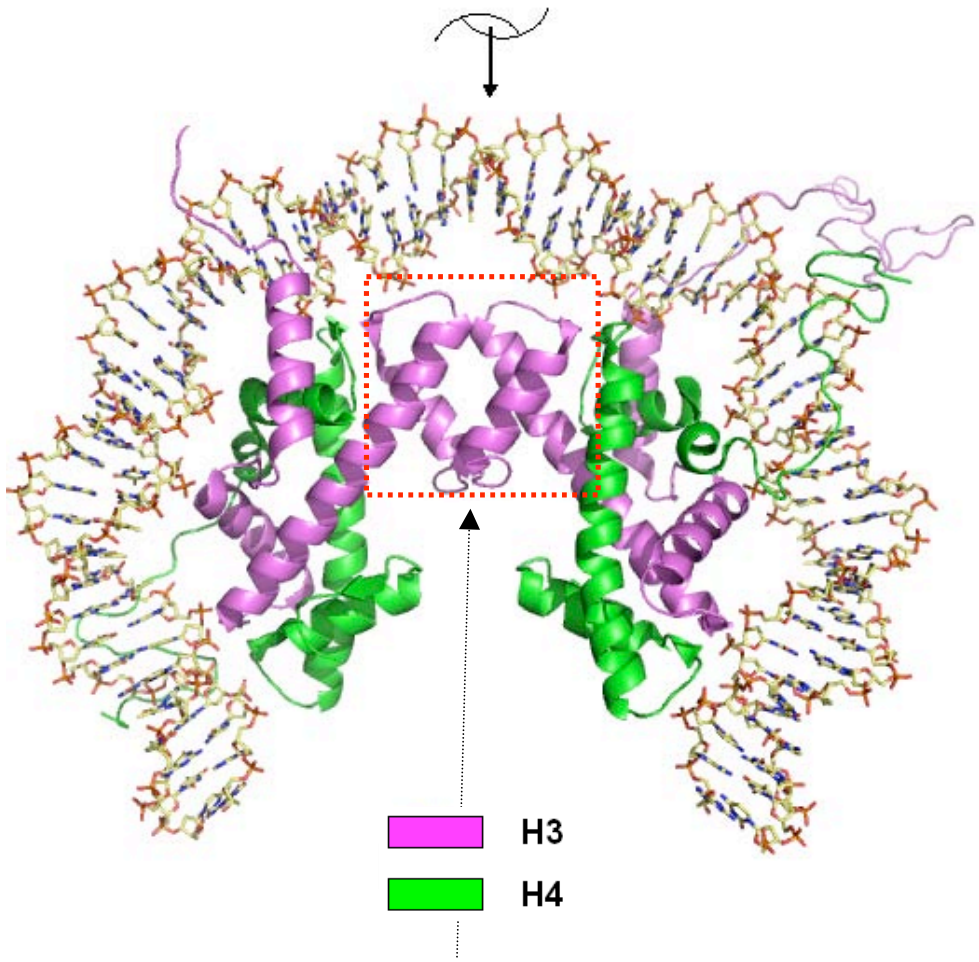

Dimeric halves stabilized through a four-helix bundle

approximate two-fold symmetry

Two H2A/H2B dimers associate with the end faces of the $(H3/H4)_2$ tetramer to form the histone octamer, around which DNA wraps.

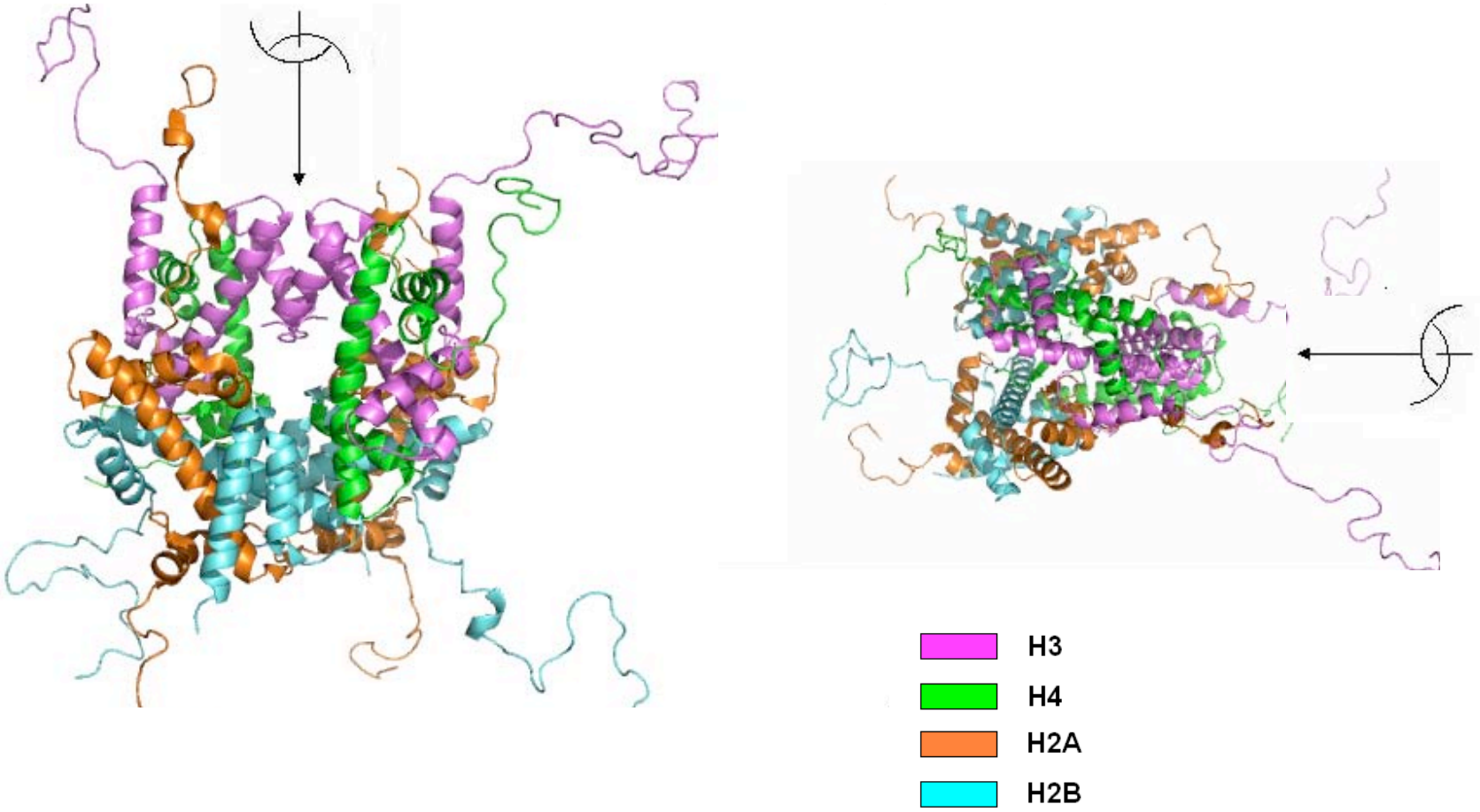

Cutting the DNA-bound octamer in half reveals the symmetry of the nucleosome.

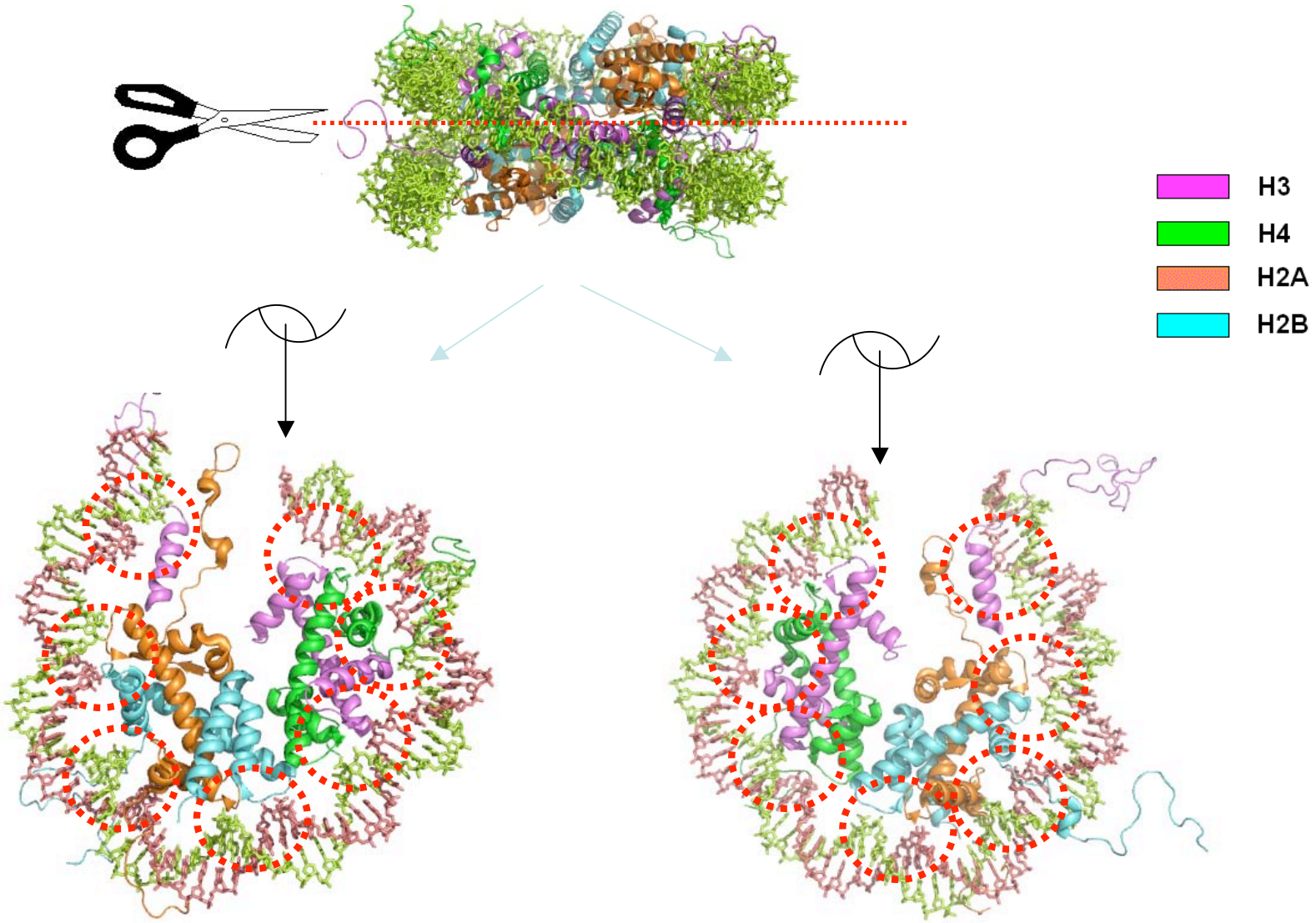

Structurally variable tails make up roughly a quarter of the histone mass.

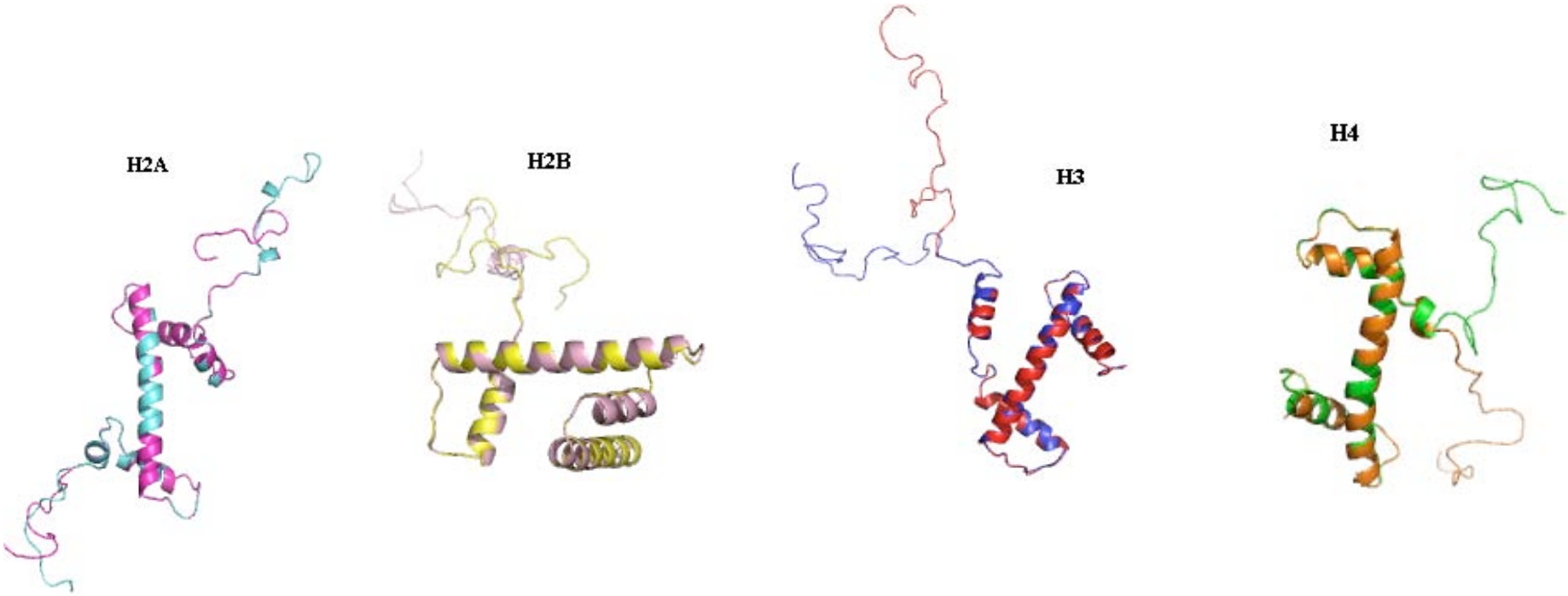

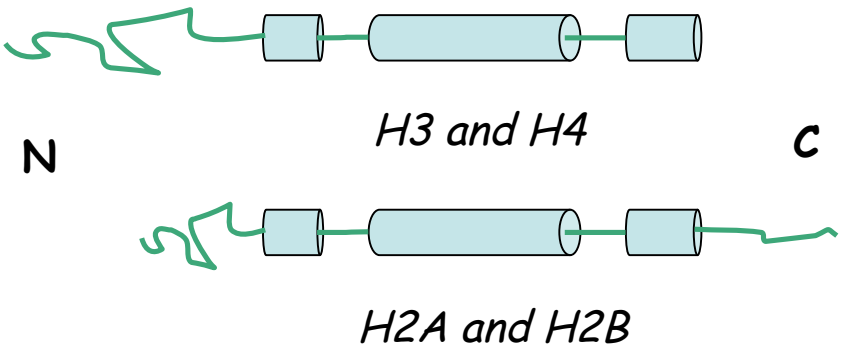

- All histones have N-terminal tails
- Only H2A and H2B have C-terminal tails

The histone tails bear a high proportion of cationic amino-acid residues.

H2A (128): SGRGKQGGKT RAKAKTRSSR AGLQFPVGRV HRLLRKGNYA ERVGAGAPVY LAAVLEYLTA EILELAGNAA RDNKKTRIIP
RHLQLAVRND EELNKLLGRV TIAQGGVLPN IQSVLLPKKT ESSKSKSK

H2B (125): PEPAKSAPAP KKGSKKAVTK TQKKDGKKRR KTRKESYAIY VYKVLKQVHP DTGISSKAMS IMNSFVNDVF ERIAGEASRL
AHYNKRSTIT SREIQTAVRL LLPGELAKHA VSEGTKAVTK YTSAK

H3 (135): ARTKQTARKS TGGKAPRKQL ATKAARKSAP ATGGVKKPHR YRPGTVALRE IRRYQKSTEL LIRKLPFQRL VREIAQDFKT
DLRFQSSAVM ALQEASEAYL VALFEDTNLC AIHAKRVTIM PKDIQLARRI RGERA

H4 (102): SGRGKGGKGL GKGGAKRHRK VLRDNIQGIT KPAIRRLARR GGVKRISGLI YEETRGVLKV FLENVIRDAV TYTEHAKRKT
VTAMDVVYAL KRQGRTLYGF GG

Table 6.1: 1-D distribution of charges on histones

Histone	Region	Total res.	Positive res. (ratio)	Negative res. (ratio)
H3	Entire	135	33 (0.24)	11 (0.081)
	Tail	36	11 (0.31)	0 (0)
H4	Entire	102	27 (0.26)	7 (0.069)
	Tail	24	10 (0.42)	1 (0.042)
H2A	Entire	128	28 (0.22)	9 (0.07)
	Tail	23	9 (0.39)	1 (0.043)
H2B	Entire	125	31 (0.25)	10 (0.08)
	Tail	29	11 (0.38)	2 (0.069)

Mapping the nucleosome on a cylinder helps to understand the organization of the protein-DNA assembly.

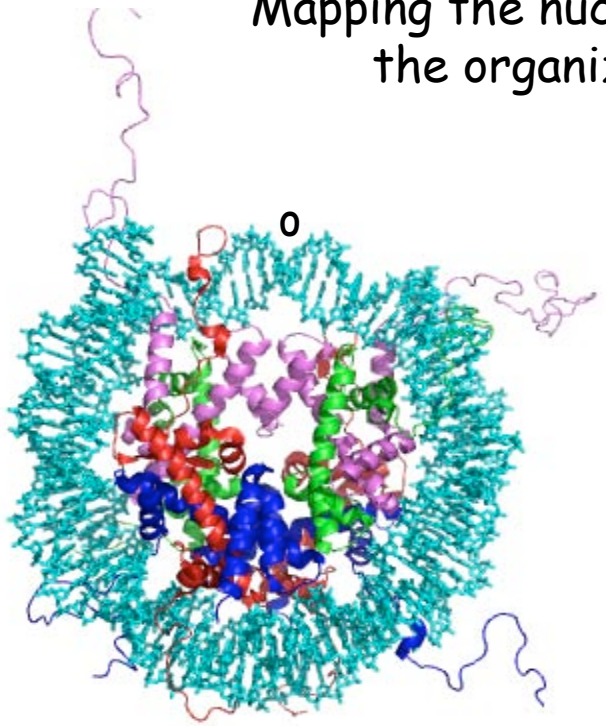

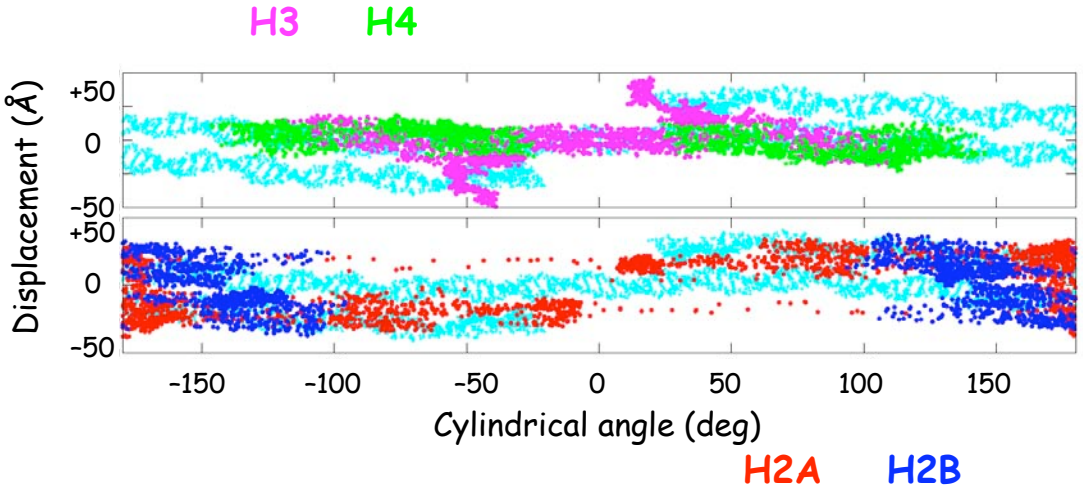

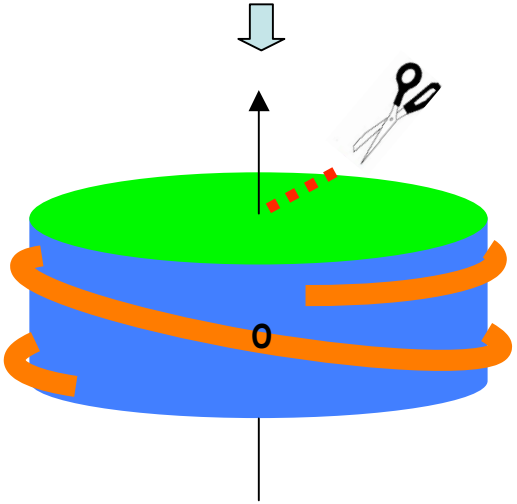

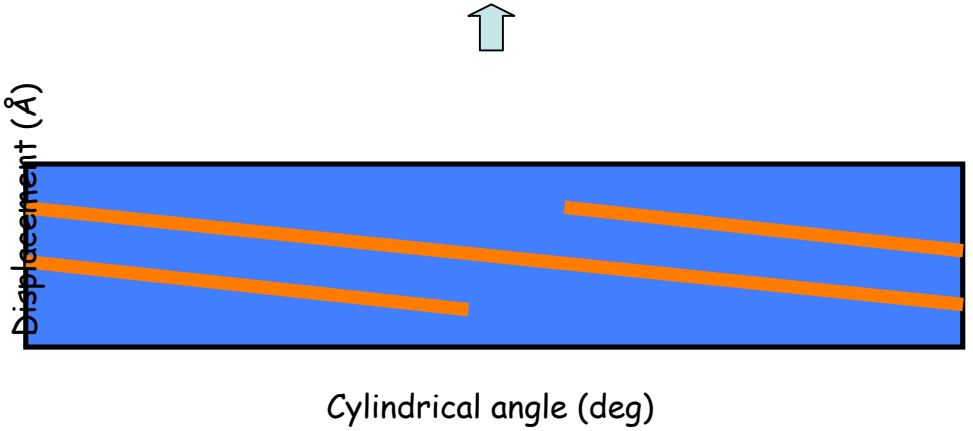

Guohui Zheng

Mapping the nucleosome core particle on a cylinder reveals 'ionic' organization in the histone interior.

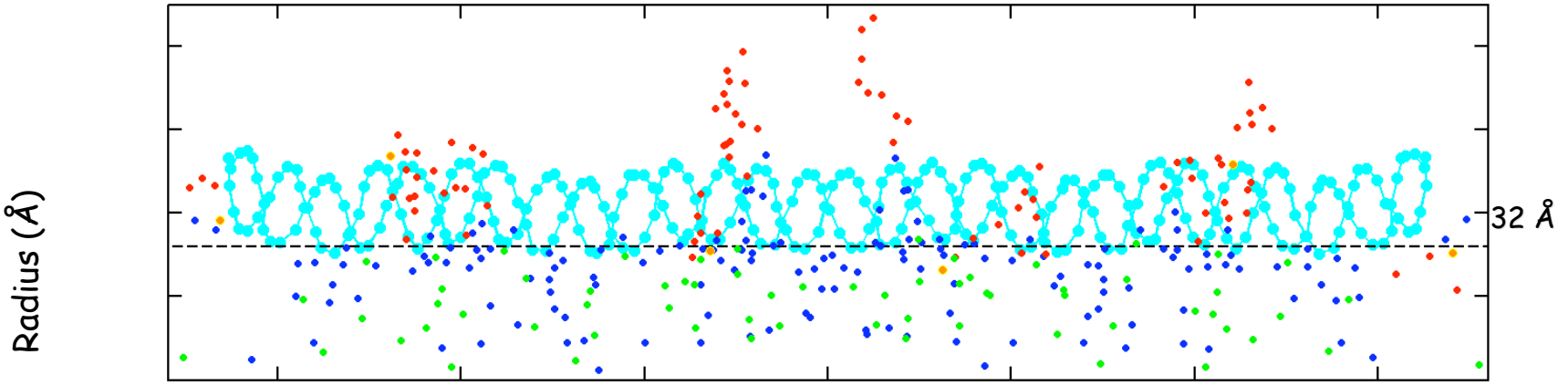

N^{1+} tails

P^{-} nucleosomal charges

O^{1-} N^{1+} core

Glu Asp Arg Lys

Guohui Zheng

Amino-acid 'cations' are neutralized by anionic residues in the histone core but exhibit a sharp build-up at the protein-DNA interface followed by a more gradual increase on the DNA exterior.

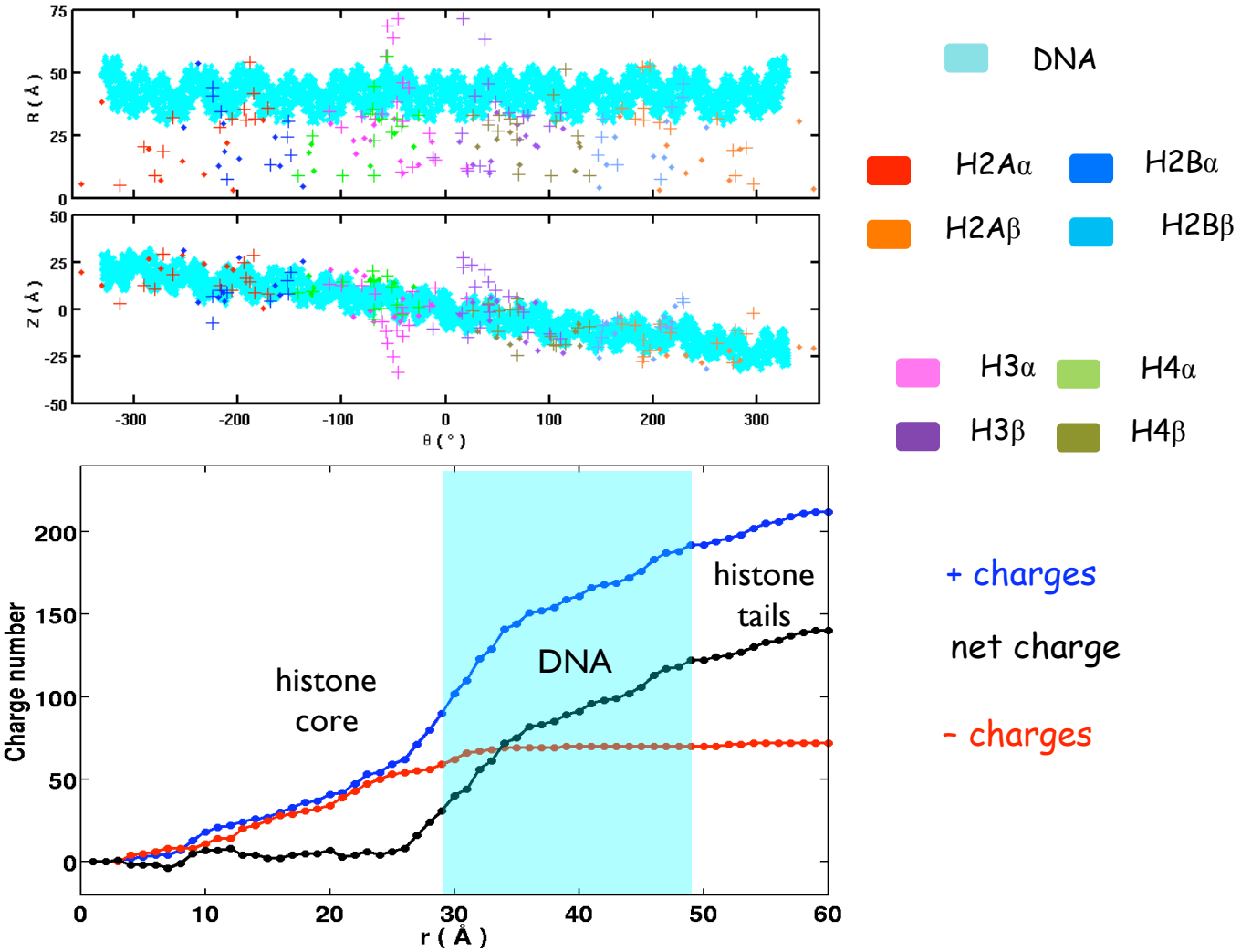

Distribution of charges within the nucleosome cylinder

Guohui Zheng

Nucleosome positioning and chromatin structure

The positioning of nucleosomes affects global chromatin folding and structure.

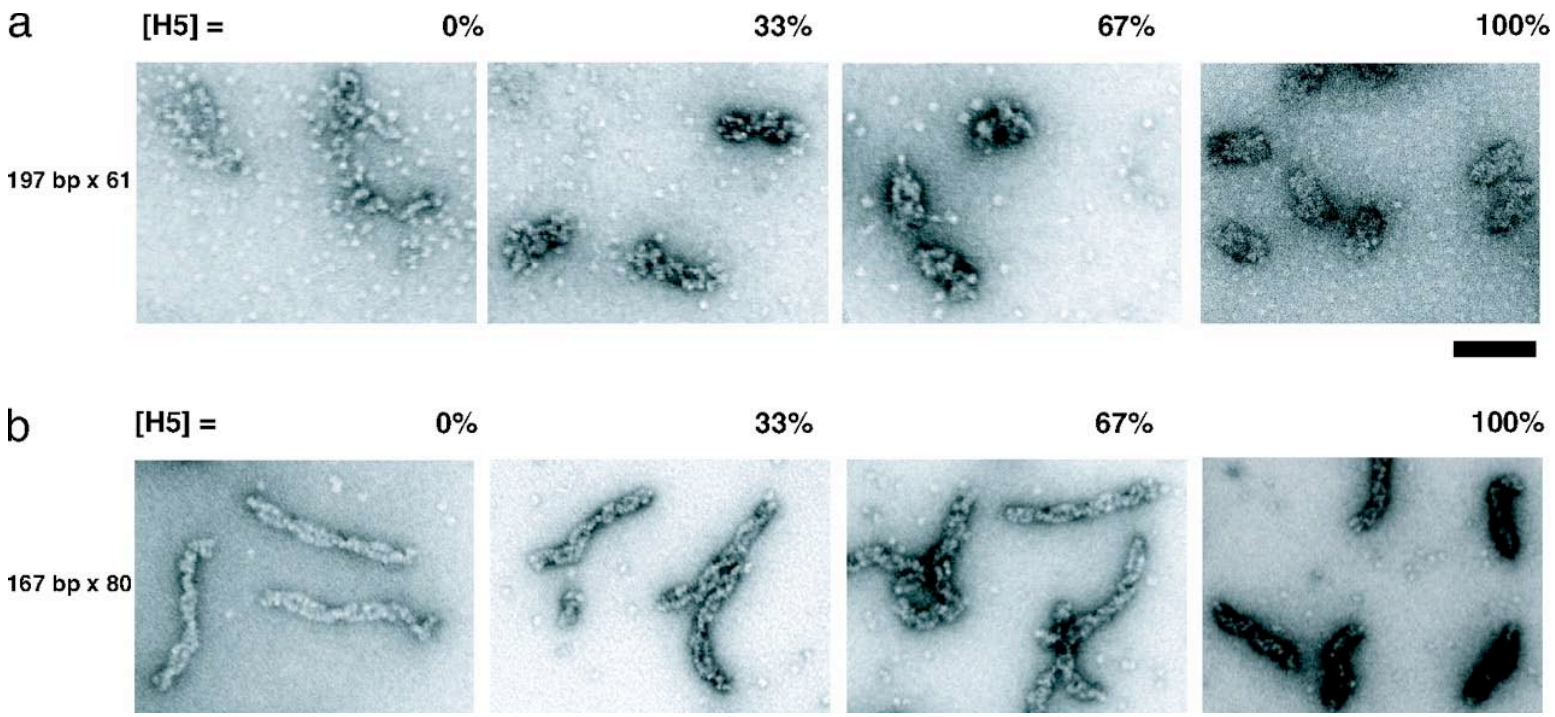

EM images reveal different linker histone-dependent folding pathways and different structures of 167- and 197-bp-repeating nucleosome arrays (with 20 and 50 bp linkers between bound nucleosomes). (a) 167-bp × 80 and (b) 197-bp × 61 nucleosome arrays reconstituted with different concentrations of linker histone (H5) and folded in the presence of 1.6 mM $MgCl_2$. Background particles are individual nucleosomes resulting from excess histone octamer bound to competitor DNA. Whereas the 197-bp arrays form regular 30-nm chromatin fibers at [H5] saturation, the 167-bp arrays form thin, more twisted, fibers.

Routh *et al.* (2009) "Nucleosome repeat length and linker histone stoichiometry determine chromatin fiber structure" *Proc. Natl. Acad. Sci., USA* 105, 8872-8877.

The positioning of nucleosomes affects global chromatin folding and structure.

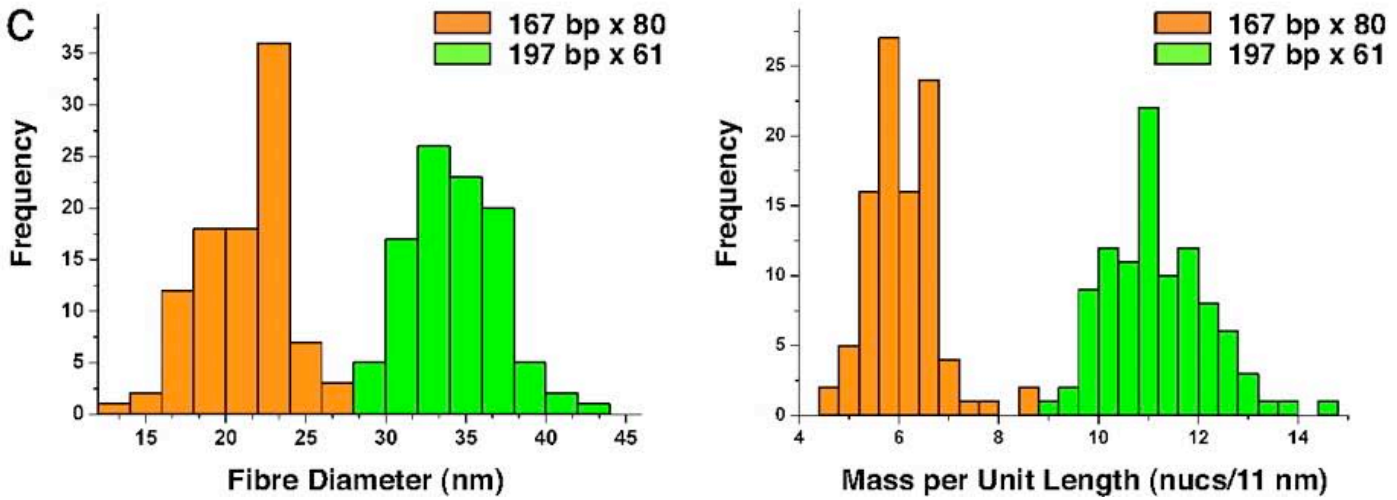

Histograms of the diameter and mass per unit length for 197-bp × 61 (green) and 167-bp × 80 (orange) fully folded chromatin fibers saturated with H5. Average diameter and mass per unit length for the 167-bp fibers are 21.3±6.1 nm and 6.1±0.74 nucleosomes per 11 nm. Corresponding values for the 197-bp fibers are 34.3±2.8 nm and 11.2±1.0 nucleosomes per 11 nm.

Routh *et al.* (2009) "Nucleosome repeat length and linker histone stoichiometry determine chromatin fiber structure" *Proc. Natl. Acad. Sci., USA* 105, 8872-8877.

The positioning of nucleosomes affects global chromatin folding and structure.

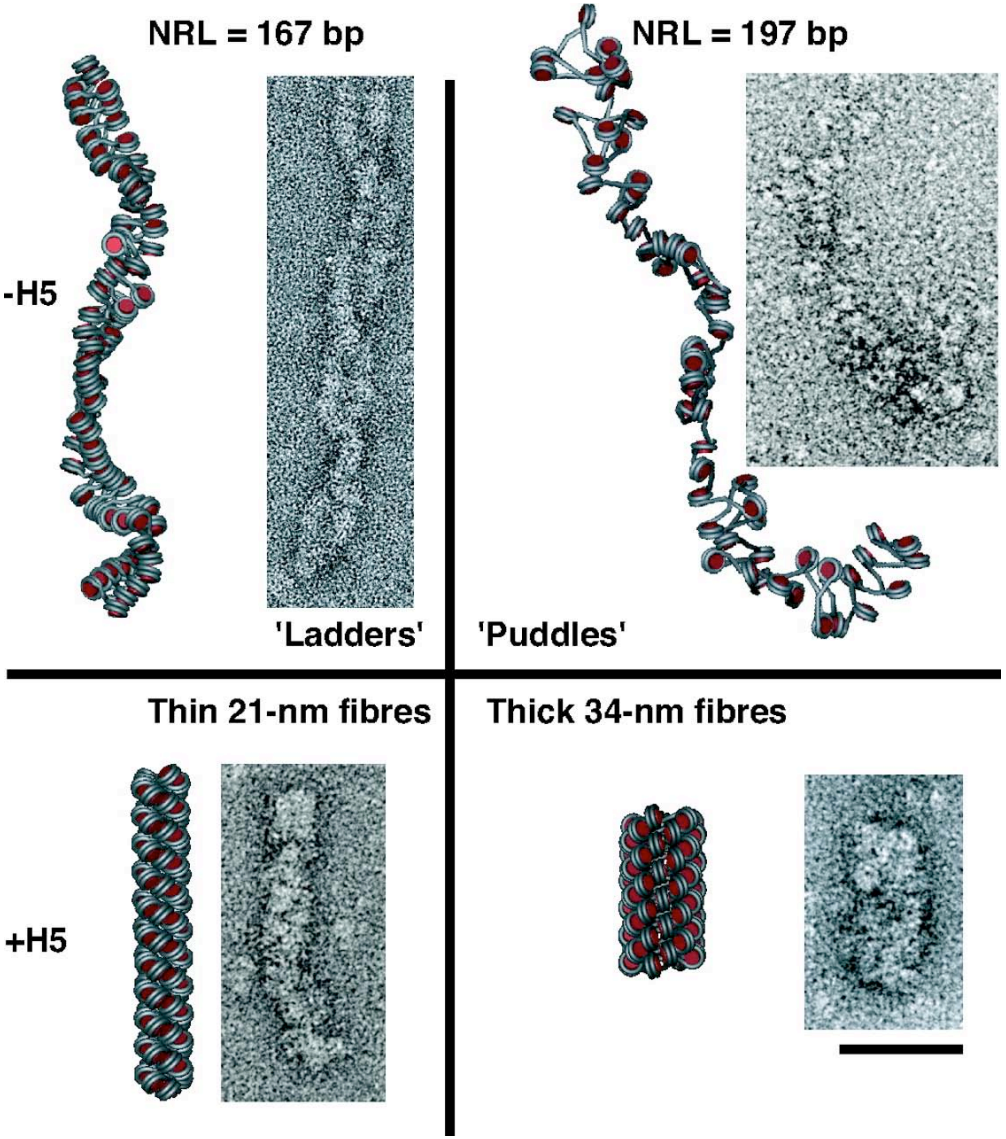

Nucleosome-repeat length and H5 determine chromatin higher-order structure.

Selected regions of EM micrographs shown next to simulated, schematic representations.

(Top left) Unfolded 167-bp array with two-start helix typified by stacking of nucleosome cores.
(Lower left) Folded 167-bp fiber in the presence of saturating H5.
(Top right) Unfolded 197-bp array showing 'puddles' in the absence of H5.
(Lower right) Folded 197-bp fiber in the presence of saturating H5.

(Scale bar: 50 nm.)

Routh *et al.* (2009) "Nucleosome repeat length and linker histone stoichiometry determine chromatin fiber structure" *Proc. Natl. Acad. Sci., USA* 105, 8872-8877.

Models of perfect, regularly spaced nucleosomes reveal the crowding of the

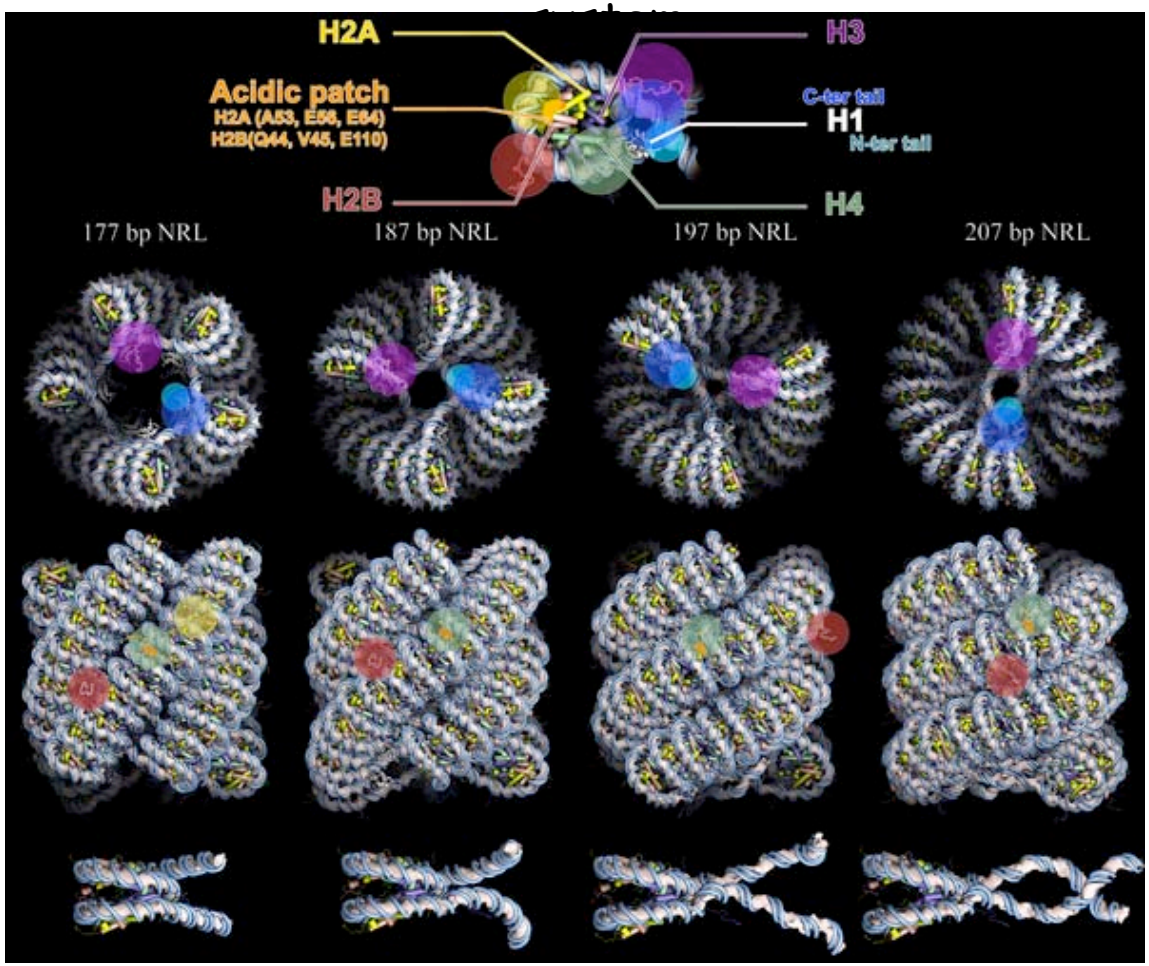

All-atom models of four H5-bound chromatin arrays with repeats of 177-207 bp. (*Top*) Color coded representation of H5 globular domain residues that interact with entry/exit DNA linkers and nucleosomal DNA at the dyad axis. (*Middle*) top and side views of models. (*Bottom*) close-up highlighting the gapping of individual nucleosomes.

Wong *et al*. (2007) "An all-atom model of the chromatin fiber containing linker histones reveals a versatile structure tuned by the nucleosomal repeat length" *PLos One* 12, e877.

Nucleosome structure and DNA deformations

The deformations of nucleosomal DNA occur at sites of close contact of protein (arginine) with the sugar-phosphate backbone.

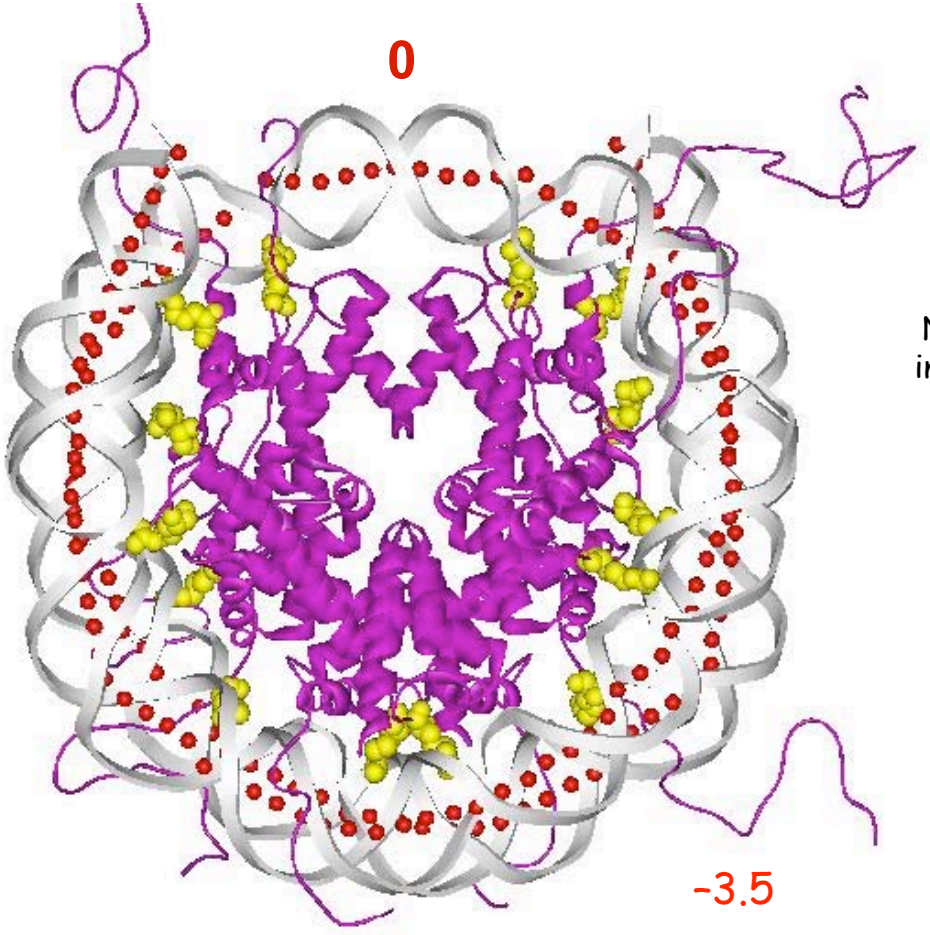

Numbers denote distance, in terms of # helical turns, of designated site from the structural dyad at 0.

bp centers

arginine

Because there are few, if any, direct contacts between the histone proteins and the DNA base atoms, the preferential 'positioning' of specific sequences on the nucleosome is thought to reflect the capability of DNA to deform along the tightly wrapped superhelical pathway.

Looking at the nucleosome from a different perspective reveals sharp jumps that accompany the bending of DNA around the histone core.

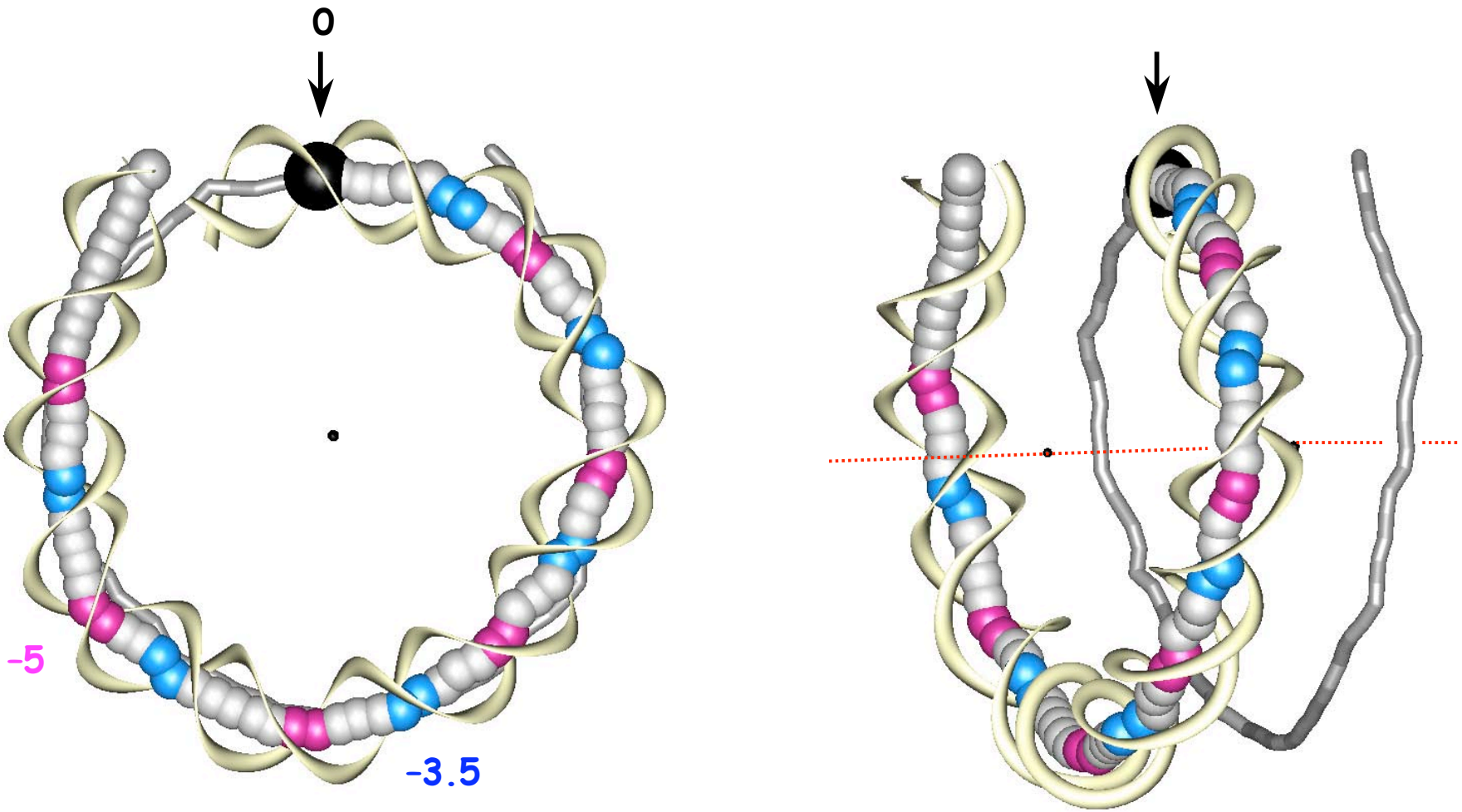

Tolstorukov et al. J, Mol. Biol. (2007)

The jumps in the superhelical pathway arise from lateral displacements that accompany the sharp bending of DNA near the sites of histone-DNA contact.

Displacement via Slide

Bending via Roll

TG:CA(38)
@ SH –3.5

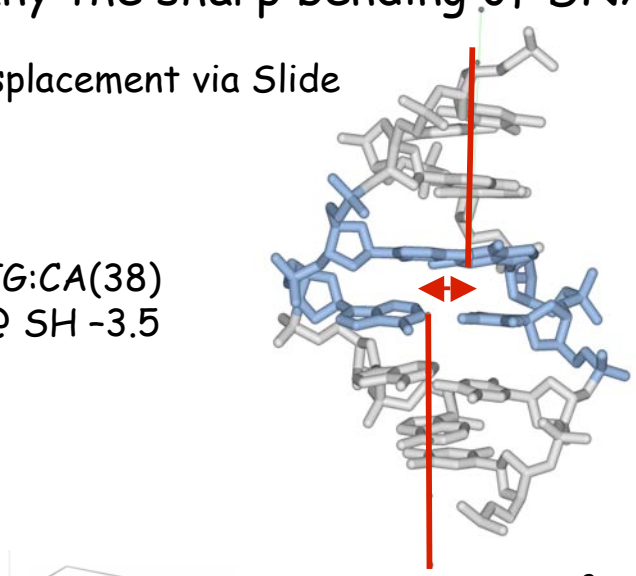

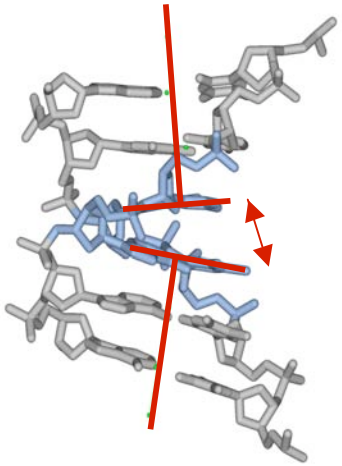

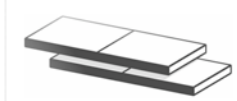

Slide = +2.7 Å
(minor-groove view)

90°

Roll = –18°
(minor-groove bend)

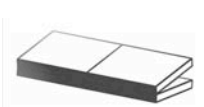

TA:TA(23)
@ SH –5

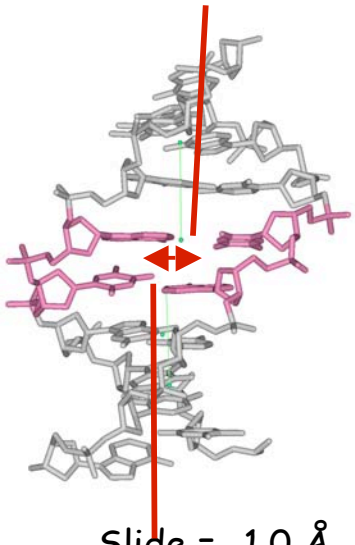

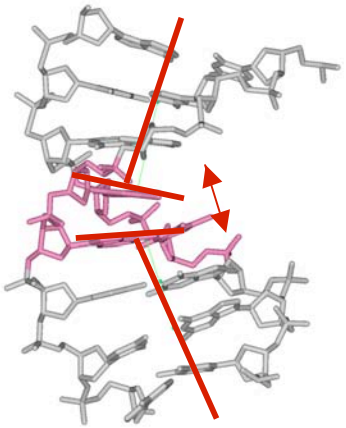

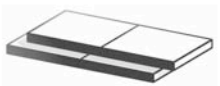

Slide = -1.0 Å
(major-groove view)

Roll = +18°
(major-groove bend)

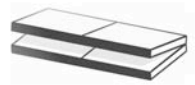

DNA deforms on the nucleosome via concerted changes of three key parameters.

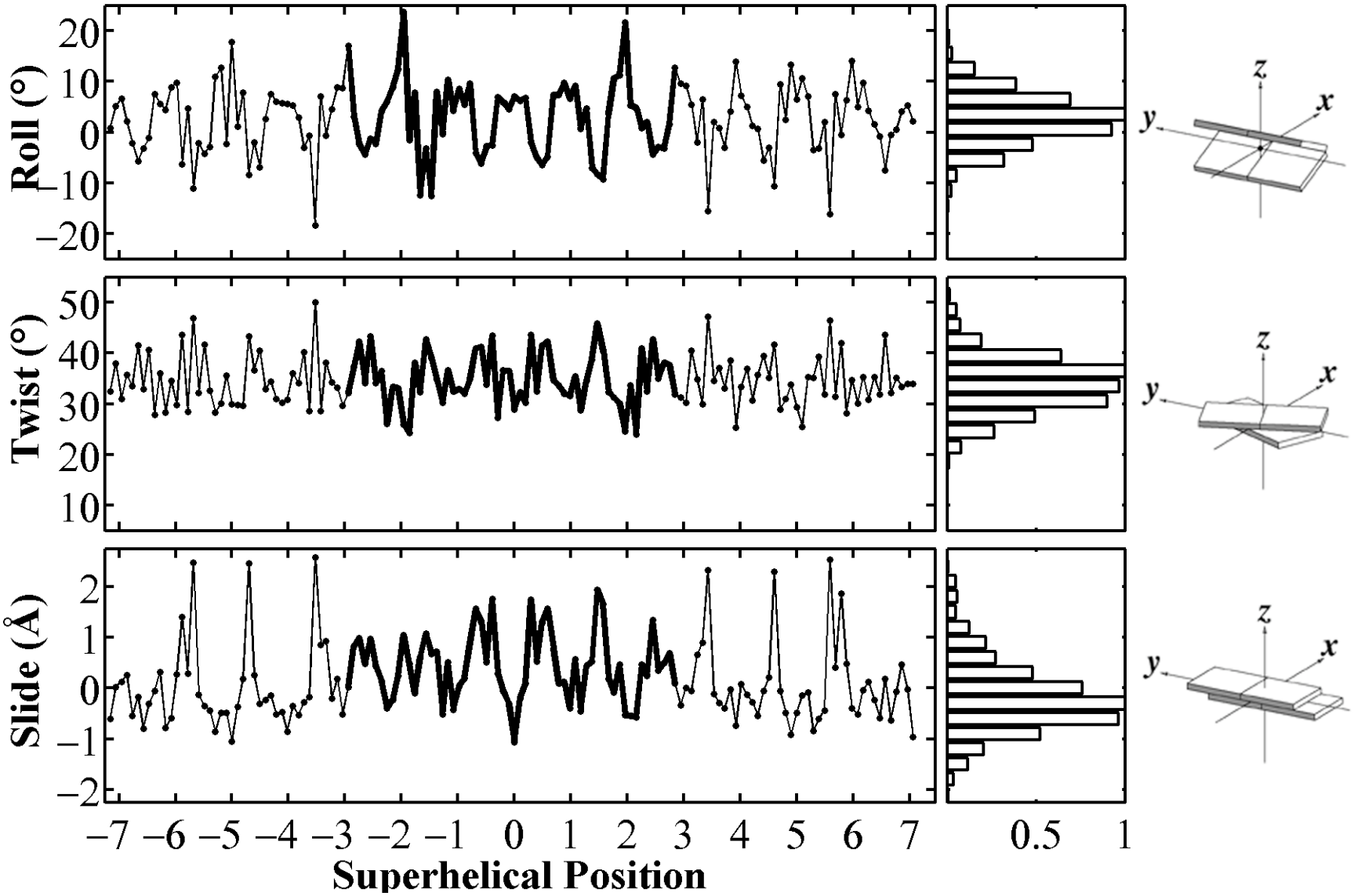

Histones: H2A-H2B; **(H3-H4)$_2$**

The two types of deformations, if repeated along the DNA, would induce well-known transitions of double-helical structure from the B to A and C forms.

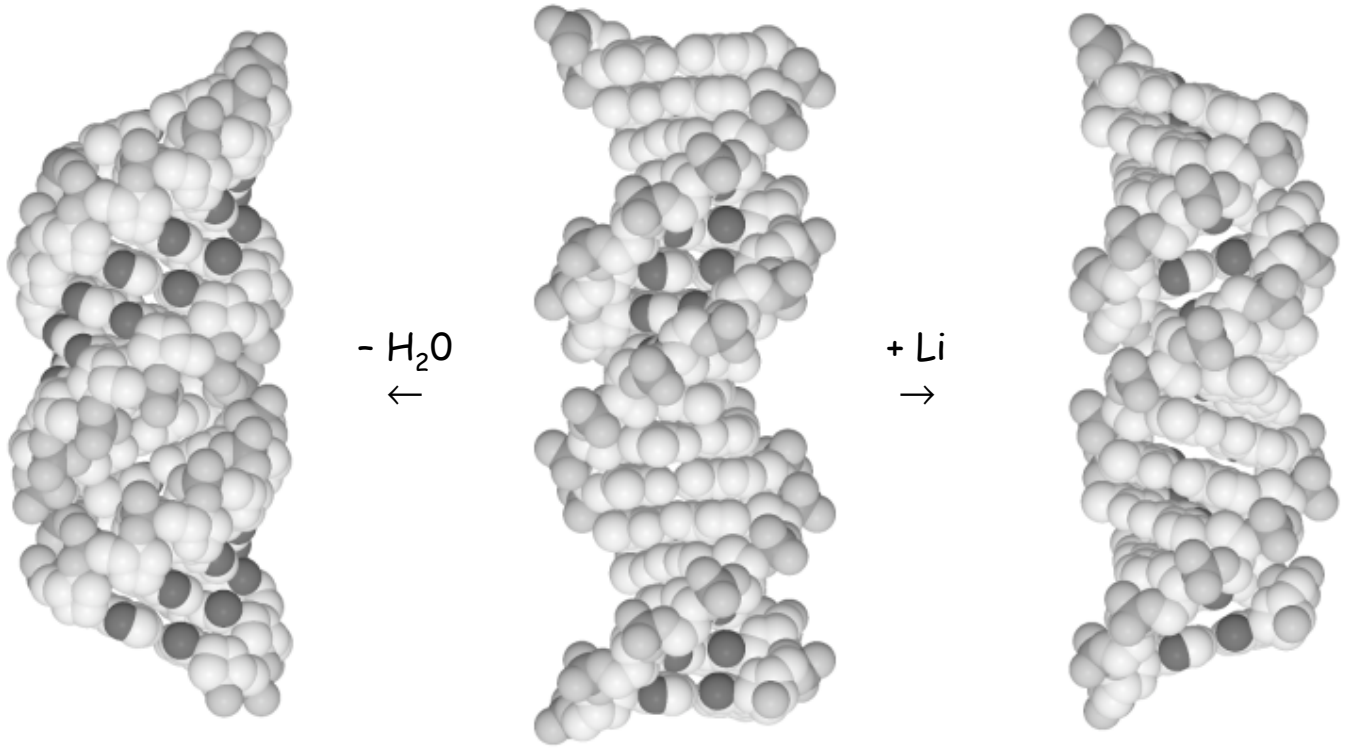

A DNA
Roll > 0
Slide < 0
11 res/turn
Narrowed M groove

B DNA
Roll ≈ 0
Slide ≈ 0
10 res/turn

C DNA
Roll < 0
Slide > 0
9 res/turn
narrowed m groove

Nucleosomal pitch is governed by Slide.

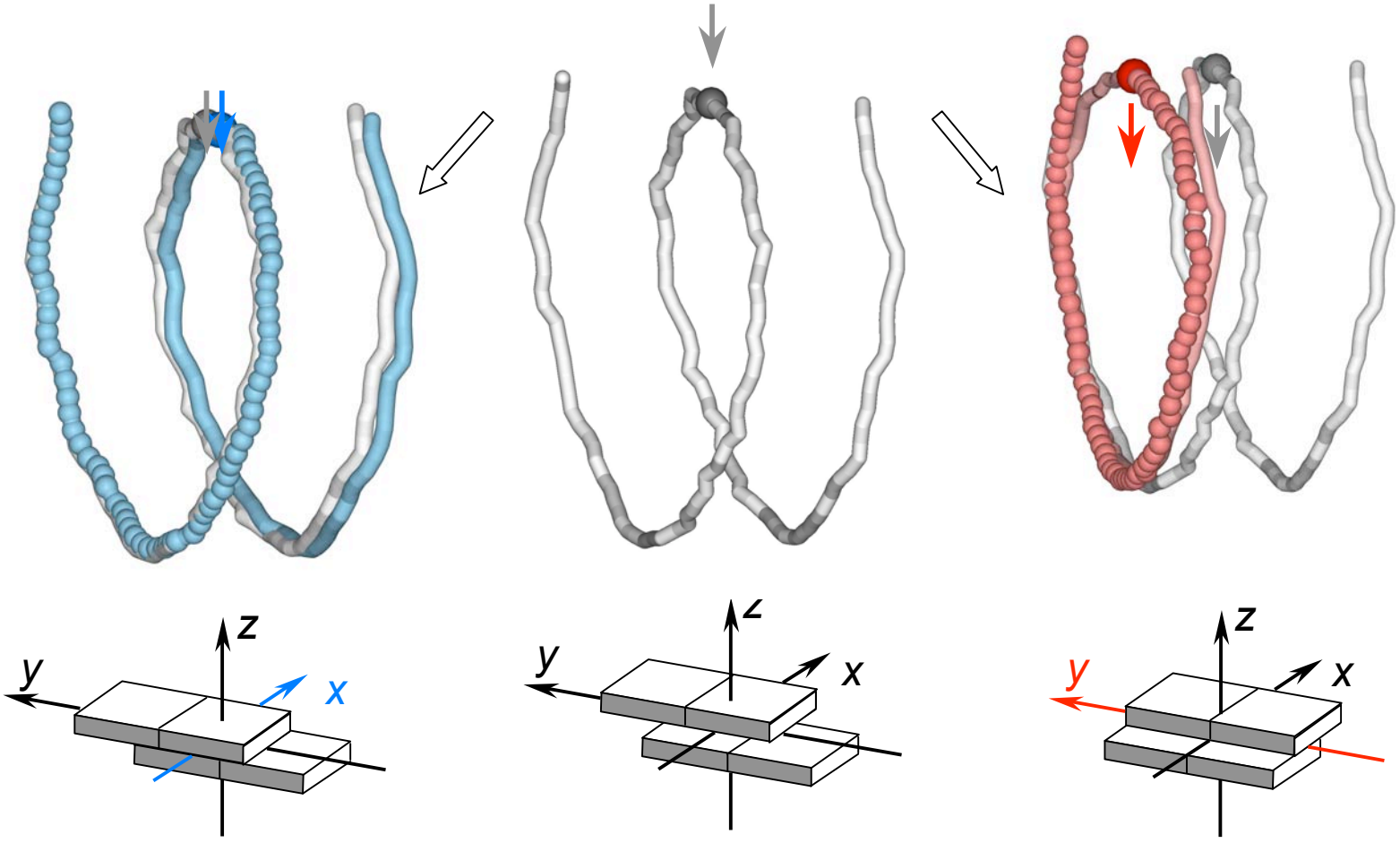

Shift = 0

Shift, Slide ≠ 0

Slide = 0

The composite changes in Slide diminish the pitch of nucleosomal DNA from ~26 Å per superhelical turn (~80 bp) in the native structure to ~3 Å in the Slide-frozen model. The effects of Shift are negligible.

The largest deformations in Slide occur at steps where the long axes of base pairs run parallel to the superhelical axis.

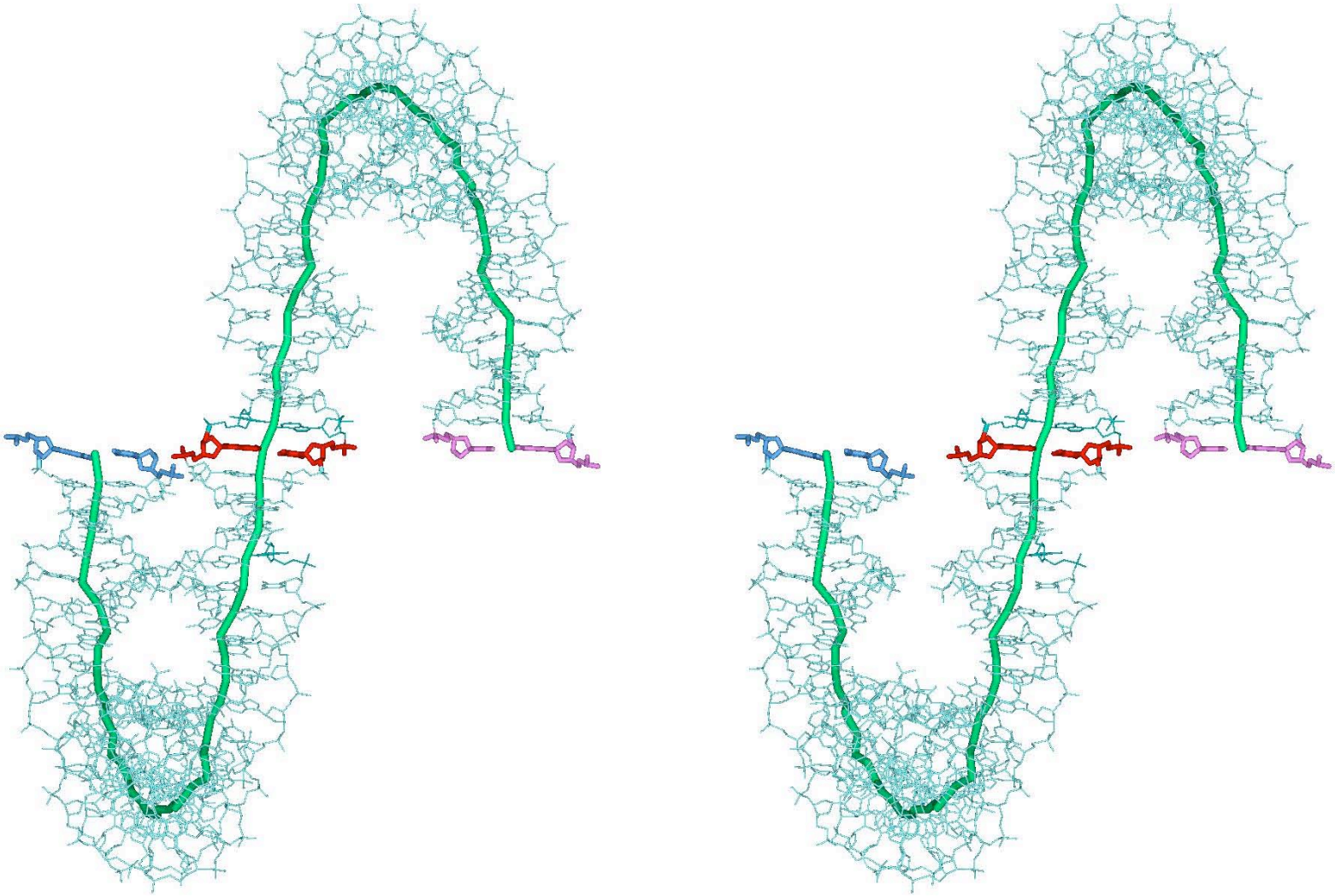

stereoview of nucleosomal DNA bps #33-115
Sl(33-34) = –0.86 Å; Sl(74) = –1.06 Å; Sl(114-115) = –0.74 Å
SH = –4 SH = 0 SH = +4

Slide accounts for > 90% of the net superhelical displacement of DNA.

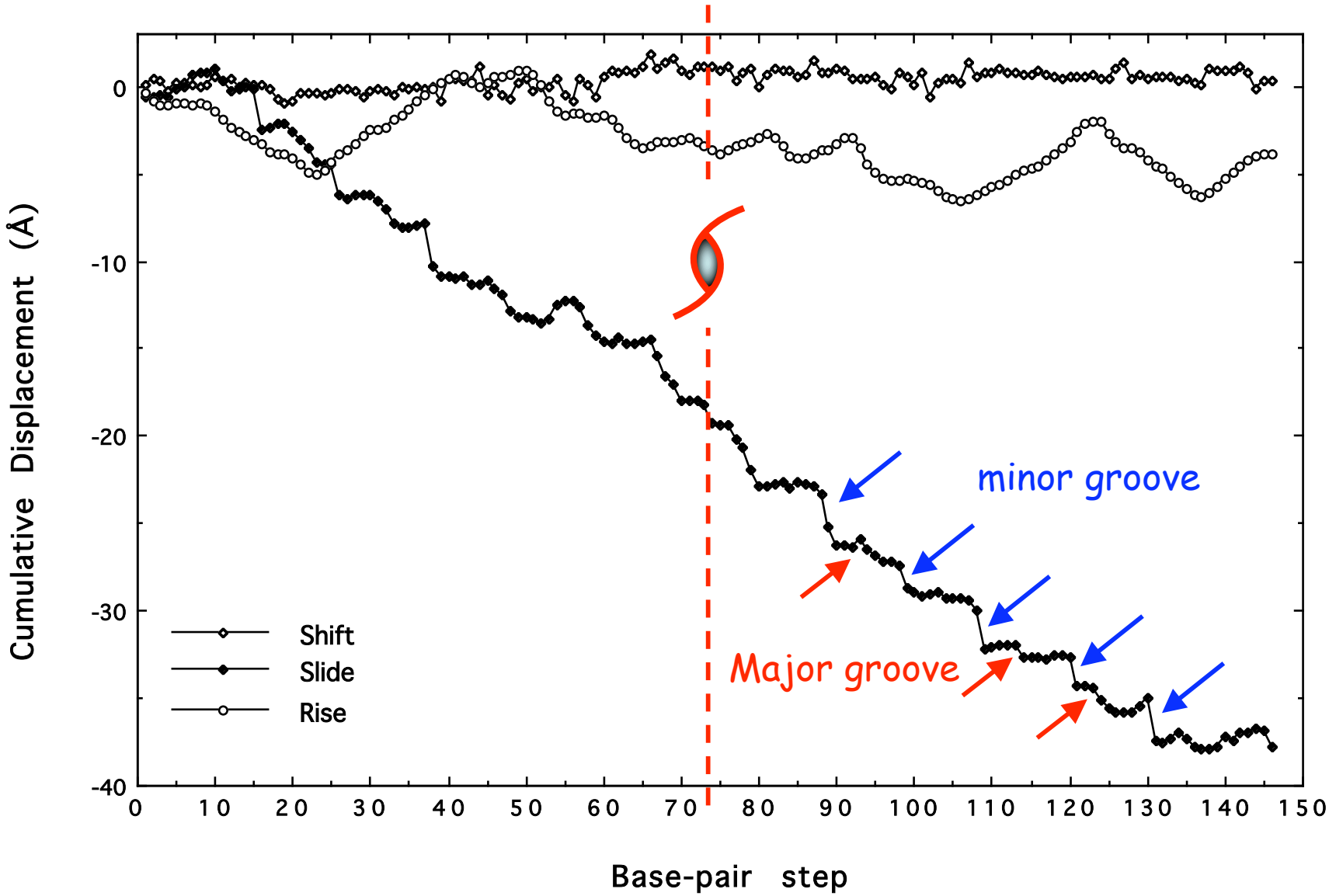

Nucleosomal DNA follows a left-handed spiral 'staircase' around the core of histone proteins.

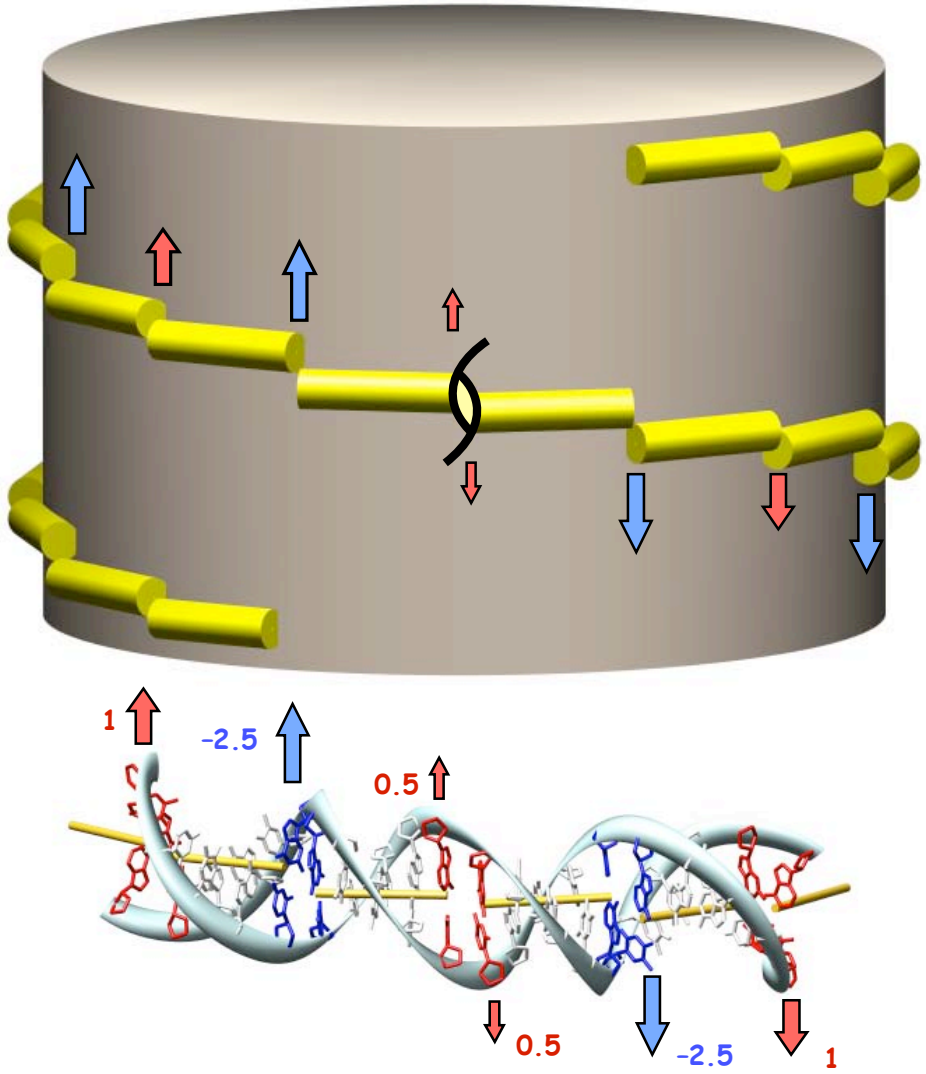

Nucleosome positioning and sequence threading

There is a noticeable minimum in the 'threading' score when the 'natural' sequence is in register with the observed structure.

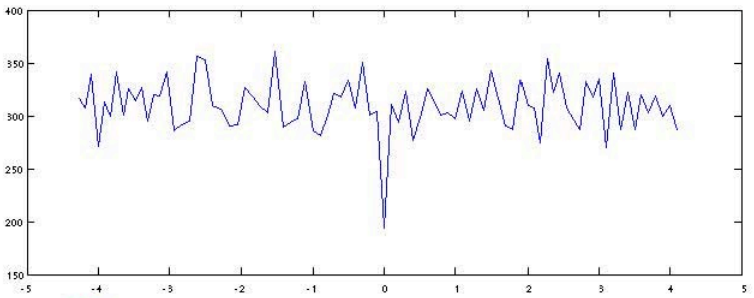

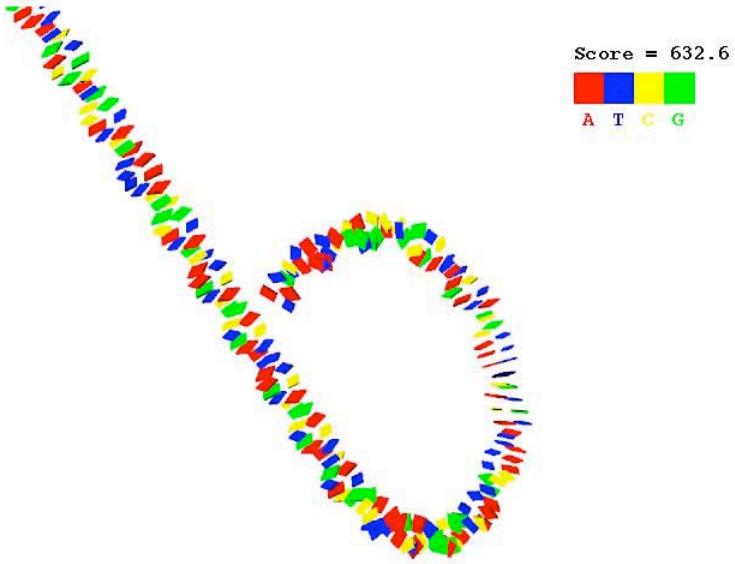

The 'threading' score reflects:

(i) setting of sequence on the structural scaffold, *i.e.*, θ_i

(ii) sequence-dependent potentials derived from the distributions of base-pair step parameters found in other high-resolution structures.

Scaffold: central 61 bp of the currently best resolved nucleosome core-particle structure (NDB_ID: pd0287; Davey *et al.*, 2002).

Sequence: human α-satellite DNA crystallized in the same structure.

'Cost' of threading base-pair steps at any position on the DNA pathway around the nucleosome core particle is lowest for pyrimidine-purine steps

Deformation 'energies' along the central 61 bp of DNA in contact with H3 and H4 proteins on either side of the nucleosomal dyad (60-bp steps) in the best-resolved nucleosome core-particle structure (PDB_ID pd0287).

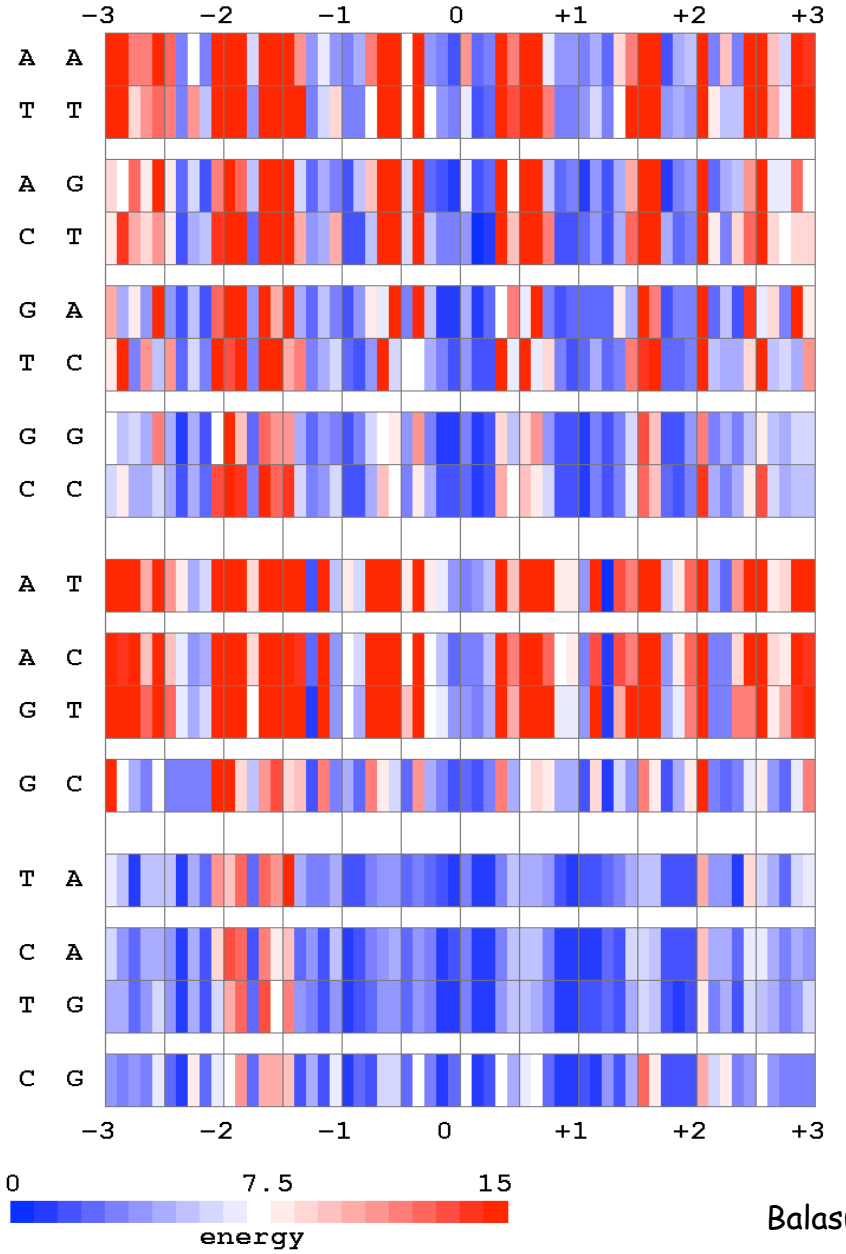

Highest barriers occur at dimer steps where Roll and Slide exhibit large, concerted deformations.

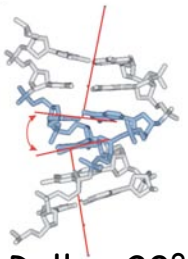

Roll < -20°

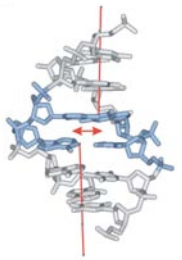

Slide > 2 Å

Balasubramanian et al. Biophys. J, (2009)

The alignment preference nearly disappears if the contribution from Slide is omitted but persists if that from Roll is removed.

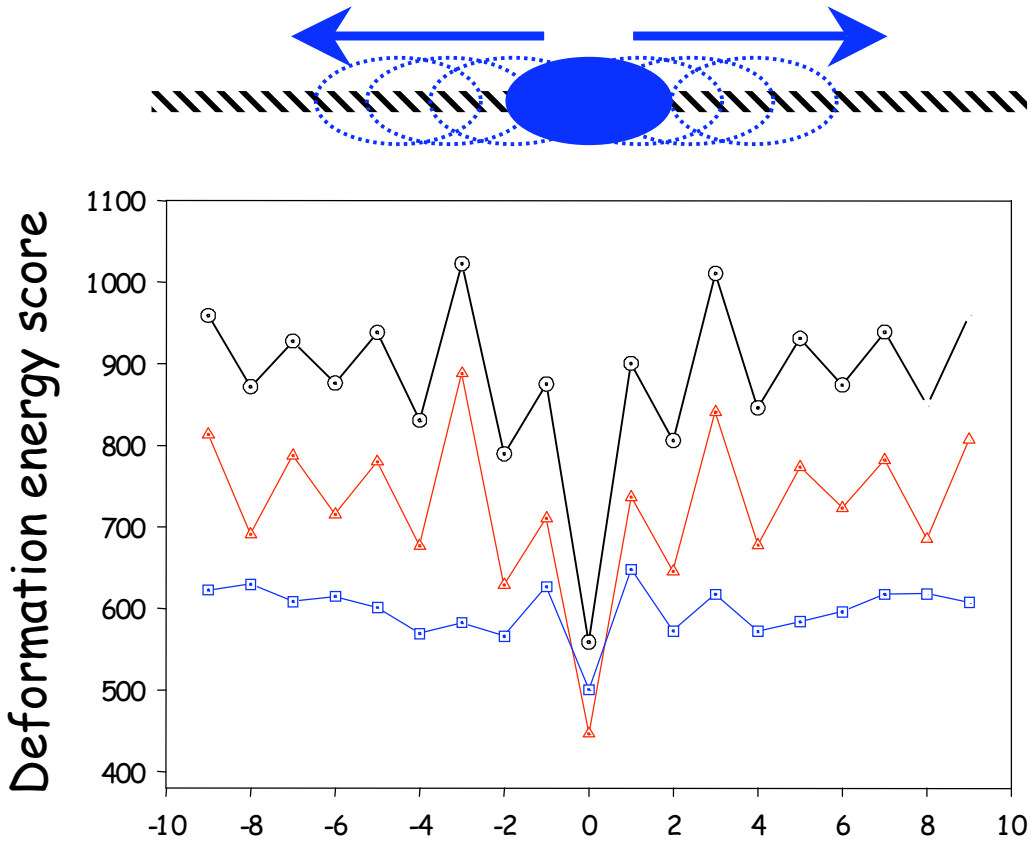

Deformation scores of 129-bp fragments of the crystallized human α-satellite sequence 'threaded' in different settings on the observed three-dimensional fold.

Tolstorukov et al. J, Mol. Biol. (2007)

The calculated threading profiles account within 1 bp for the positioning of DNA on well characterized nucleosomes.

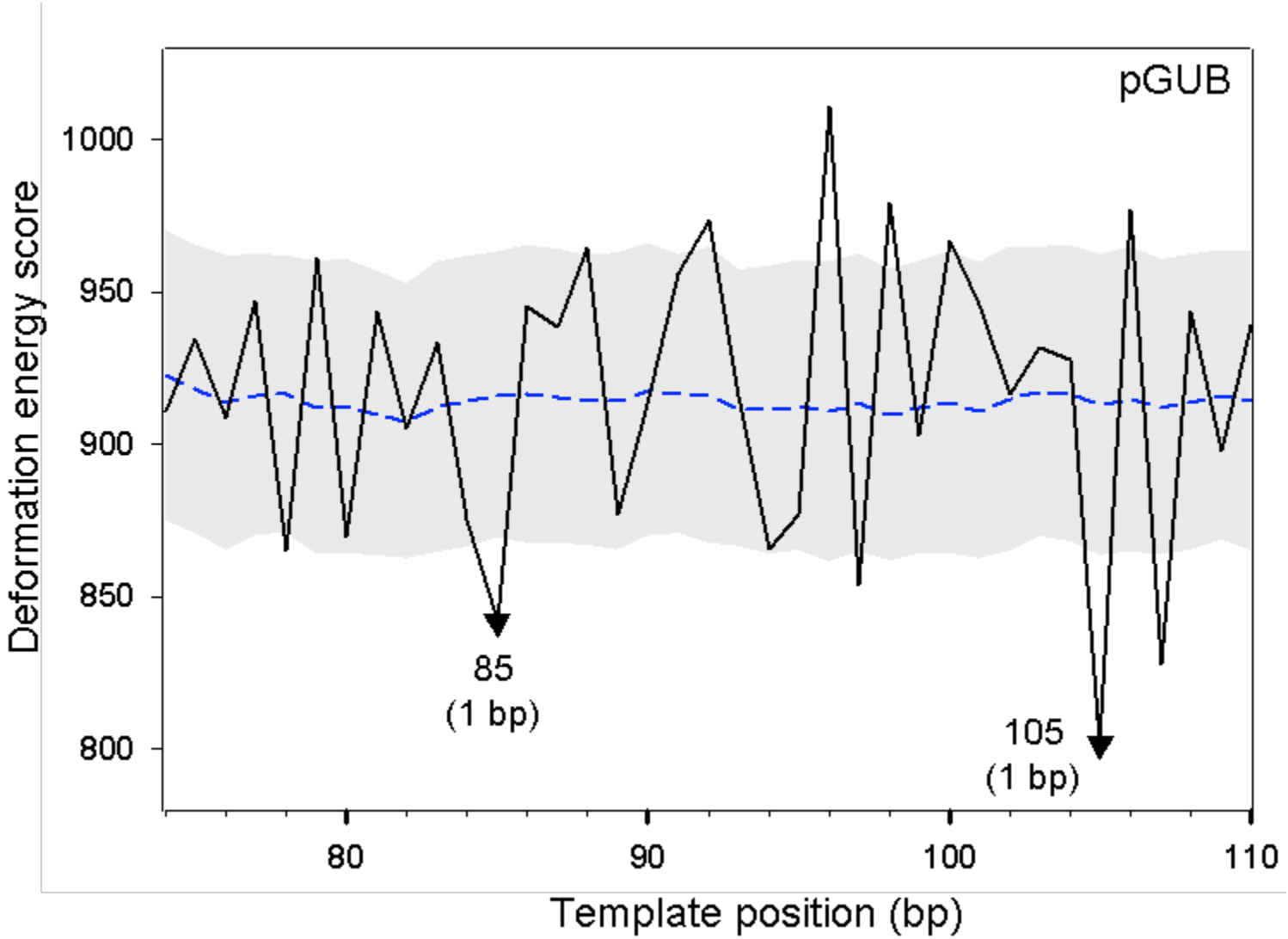

Tolstorukov et al. J, Mol. Biol. (2007)

DNA supercoiling

DNA in biological systems is typically supercoiled.

The secondary (double helical) and tertiary (folded) structure of DNA are interdependent if the chain is supercoiled by constraining the molecule to configurations other than the natural (relaxed) state. Such states include the arrangements of DNA constrained by containment in a viral capsid, the looping of DNA mediated by proteins, the wrapping of nucleosomal DNA, or combinations thereof.

Linking number *Lk*: a topological invariant defined by the interplay of secondary and tertiary structure.

Writhing number *Wr*: a measure of the folding of the double helical axis obtained by various methods, such as the average number of signed chain crossings in a closed duplex observed from all possible directions.

Twist number *Tw*: the total twisting of successive base pairs about the helical axis, expressed in terms of the number of helical turns.

$$Lk = Wr + Tw$$

The global bending and twisting of supercoiled DNA are interdependent.

$$Lk = Wr + Tw$$

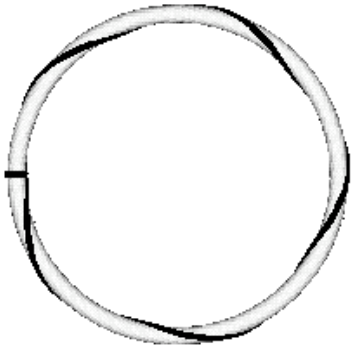

Lk = 5
Wr = 0
Tw = 5

Lk = 5
Wr = 1
Tw = 4

Lk = 5
Wr = 2
Tw = 3

The writhing number depends on the overall pathway of the DNA axis.

Conceptual definition of the writhing number

1. Project the configuration of the DNA chain onto a plane perpendicular to a specific viewing direction ω.
2. Score each region of chain self-overlap in projection as +1 or –1 depending on the handedness of the crossing.
3. Sum the scores to determine the directional writhing number $Wr(\omega)$.
4. Repeat steps 1-3 for all possible viewing directions.
5. Calculate the writing number as the average value of the directional writhing numbers.

The sign of the directional writhing number is the same as that of the vector triple product:

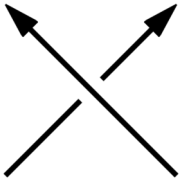

$$\left[\left(\mathbf{r}_{i+1}-\mathbf{r}_i\right)\times\left(\mathbf{r}_{j+1}-\mathbf{r}_j\right)\right]\cdot\left(\mathbf{r}_i-\mathbf{r}_j\right)$$

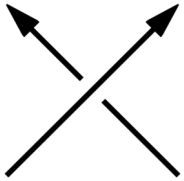

negative crossing

positive crossing

Fuller (1971) "The writhing number of a space curve." *Proc. Natl. Acad. Sci., USA* 68,, 815-819.

The writhing number can also be defined as the fraction of viewing directions along which pairs of line segments *i—i+1* and *j—j+1* are seen to overlap.

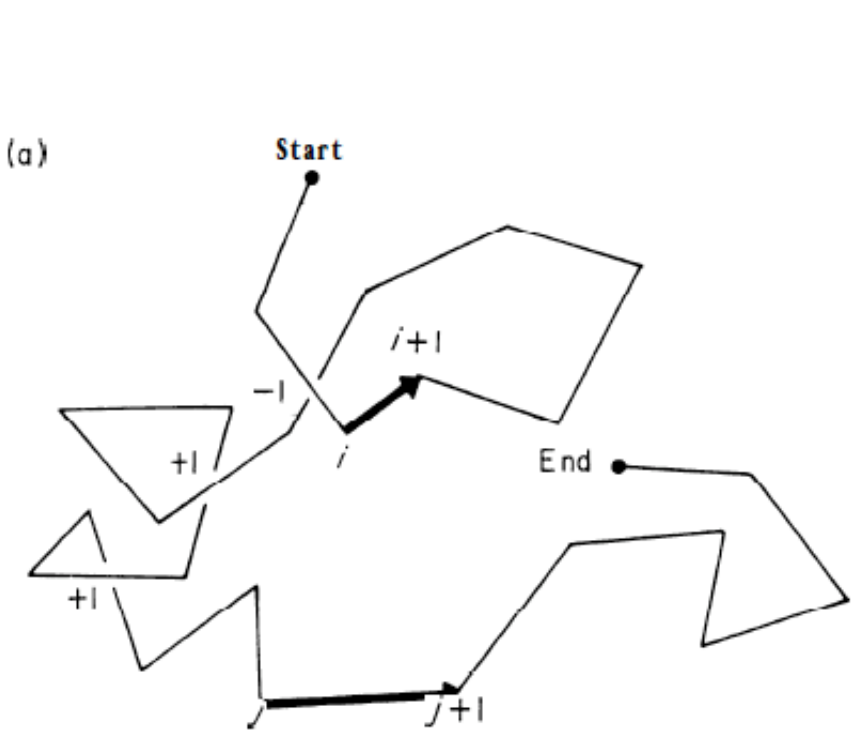

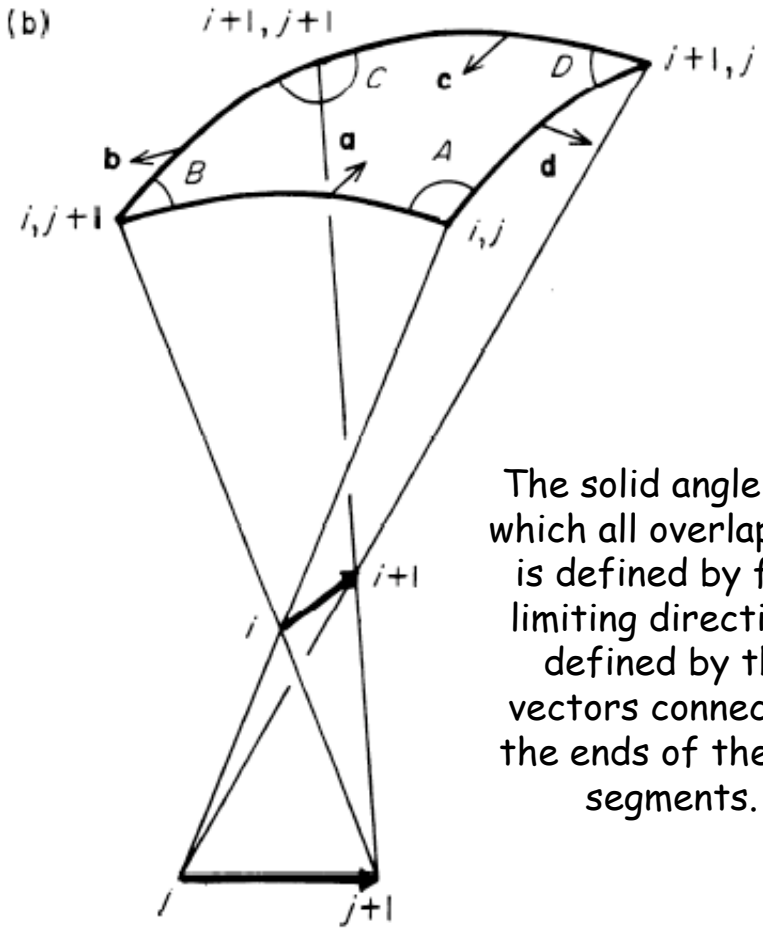

The solid angle Ω in which all overlaps lie, is defined by four limiting directions, defined by the vectors connecting the ends of the two segments.

Levitt (1983) "Protein folding by restrained energy minimization and molecular dynamics." *J. Mol. Biol.* 170, 723-764.

The writhing number is a sum of the fraction of overlapped viewing directions for all pairs of line segments.

$$Wr = \sum_{i,j>i}^{n} Wr_{ij}$$

$$Wr_{ij} = 2\Omega_{ij} \Big/ 4\pi$$

Wr_{ij} is the fraction of viewing directions along which line segments i—i+1 and j—j+1 overlap.

$$\Omega_{ij} = A + B + C + D - 2\pi$$

$$\mathbf{a} = \left(\mathbf{r}_i - \mathbf{r}_{j+1}\right) \times \left(\mathbf{r}_i - \mathbf{r}_j\right)$$
$$\mathbf{b} = \left(\mathbf{r}_i - \mathbf{r}_{j+1}\right) \times \left(\mathbf{r}_{i+1} - \mathbf{r}_{j+1}\right)$$
$$\mathbf{c} = \left(\mathbf{r}_{i+1} - \mathbf{r}_j\right) \times \left(\mathbf{r}_{i+1} - \mathbf{r}_{j+1}\right)$$
$$\mathbf{d} = \left(\mathbf{r}_{i+1} - \mathbf{r}_j\right) \times \left(\mathbf{r}_i - \mathbf{r}_j\right)$$

$$A = \cos^{-1}\left(\mathbf{a} \cdot \mathbf{d} \Big/ \left|\mathbf{a}\right|\left|\mathbf{d}\right|\right)$$
$$B = \cos^{-1}\left(\mathbf{b} \cdot \mathbf{a} \Big/ \left|\mathbf{b}\right|\left|\mathbf{a}\right|\right)$$
$$C = \cos^{-1}\left(\mathbf{c} \cdot \mathbf{b} \Big/ \left|\mathbf{c}\right|\left|\mathbf{b}\right|\right)$$
$$D = \cos^{-1}\left(\mathbf{d} \cdot \mathbf{c} \Big/ \left|\mathbf{d}\right|\left|\mathbf{c}\right|\right)$$

The angles (A, B, C, D) of the spherical quadrilateral are obtained from the vectors (**a**, **b**, **c**, **d**) which point toward the poles of the great circles forming the sides of the quadrilateral.

Levitt (1983) "Protein folding by restrained energy minimization and molecular dynamics." *J. Mol. Biol.* 170, 723-764.

The twist of supercoiling *Tw* measures the intertwining of two smooth space curves, one representing one of the DNA strands and the other the helical axis.

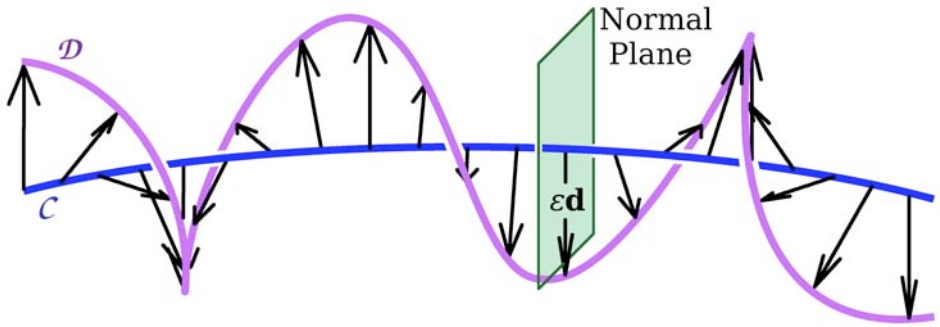

Schematic representation of DNA, with the double-helical axis given by curve *C* and one of the helical strands by curve *D*. For purposes of determining the twist of *D* about *C*, *D* is thought of as being traced out by the head of a vector $\varepsilon\mathbf{d}$ everywhere perpendicular to the tangent of curve *C*.

$$Tw(D,C) = \left(\frac{1}{2\pi}\right)\int_{s_{C_1}}^{s_{C_2}} \mathbf{t}_C\left(s_C\right)\cdot\left(\mathbf{d}\left(s_C\right)\times d\mathbf{d}\left(s_C\right)\right)$$

Tobias *et al.* (2009) "Two perspectives on the twist of DNA." eprint arXiv:0903.1657.

The twist of supercoiling differs from the step-parameter twist, in being sensitive to chiral structural distortions.

(a) Four equally spaced, parallel base-pair planes with origins lying on a line; (b) structure generated by introducing a bend uniformly between bases 2 and 3 (the four origins remain coplanar, and the viewing direction is normal to this plane).

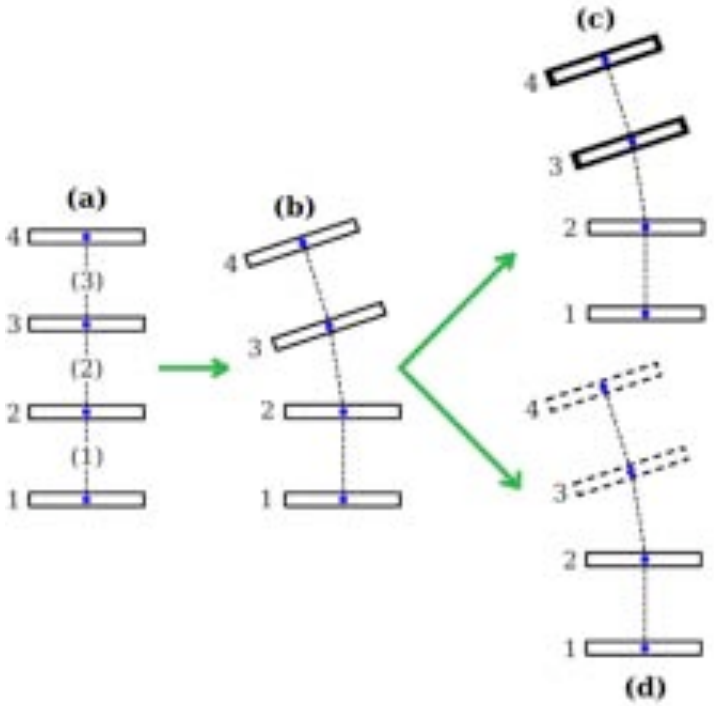

Translation of base pairs 3 and 4 as a unit along the viewing direction, depending on the direction of displacement, results either in (c), a structure with a right-handed jog, or (d), one with a left-handed jog.

Construction of a model DNA structure characterized by a chiral deformation

Tobias *et al.* (2009) "Two perspectives on the twist of DNA." eprint arXiv:0903.1657.

The twist of supercoiling of DNA bound to Tc3 transposase (PDB ID: 1tc3) is consistently lower than than of the step parameter twist and markedly so at the 5´-end of the complex where the DNA assumes an A-like form.

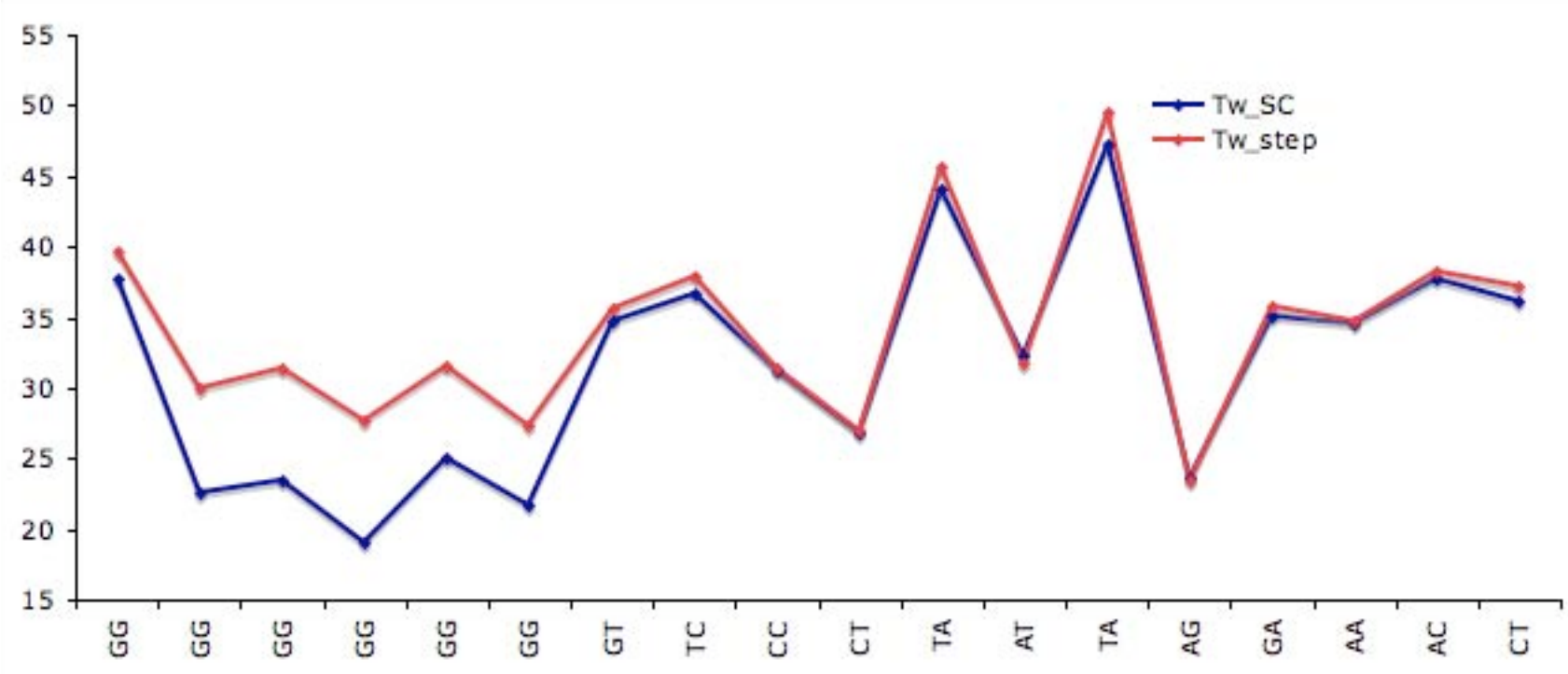

$$\sum Tw_{SC} = 569.5^\circ \text{ (1.58 helical turns)}$$

$$\sum Tw_{steo} = 615.5^\circ$$

$$18 \text{ steps} \times \left(\frac{360^\circ}{10.5} \right) = 617.1^\circ$$

Parameters taken from Lauren Britton's Twist of DNA Data Log database/search engine: http://twiddl.rutgers.edu/.